reaction barriers to a state correlation diagram,[26] These data illustrate the difficulty of interpreting a linear relationship between reaction barriers and singlet-triplet excitation energies.

**Conclusions.** Thermodynamic considerations require that the energetics involved in association of ground-state and dissociation of excited-state reactants be taken into account when formulating initial gaps for excitation of ground-state to excited-state complexes from ionization potentials, electron affinities, and singlet-triplet excitation energies of molecules. If the association of reactants, alone, is considered, the erroneous conclusion that since the association energy is negligibly small, the association constants can be neglected may appear reasonable. However, it is not a single association constant but rather the ratio $K^*/K^\circ$ that determines the magnitude of the effect. It is not acceptable to neglect this term without attempts to evaluate its magnitude.

Our overall conclusion is that when linear correlations between observed activation barriers and $I_D - E_A$ or $\Delta E_{ST}(\pi\pi^*)$ are found, the significance of the correlation parameters is usually not obvious. The uncertainties in the initial gap arising from the neglect of the association constants may explain the apparent failure[16,27] of the CM model analysis to correctly predict the barrier for the reaction of 9-phenylanthracene cation radical with pyridine. Further work is required to clarify the energetics of this and other ion-radical reactions.

Once again, the arguments presented in this paper are restricted to the terms that must be taken into consideration for the initial gap for excitation of ground-state donor-acceptor complexes to the corresponding excited states. The uncertainties that may arise can render the CM model analysis inappropriate for semiquantitative estimation of the reaction barrier. However, this added uncertainty is not expected to affect the qualitative use of the theory.

(26) In order to observe "reasonable" values of $f$ and $B$, the $K^*/K^\circ$ term would have to be significantly large. For example, considering only the data for benzene and anthracene, log $(K^*/K^\circ)_{ST}$ values of 24 and 4, respectively, would give rise to $f = 0.25$ and $B = 2.9$. This implies a linear relationship between log $(K^*/K^\circ)_{ST}$ and $\Delta E_{ST}(\pi\pi^*)$ with a slope equal to 0.48.

(27) Parker, V. D.; Tilset, M. *J. Am. Chem. Soc.* **1987**, *109*, 2521.

## Experimental Section

**Reagents.** Benzenediazonium tetrafluoroborate was prepared by a standard procedure,[28] recrystallized from dry methanol and ether, and stored at −5 °C. Tetrabutylammonium tetrafluoroborate (Aldrich) was used as received. Dichloromethane was distilled over calcium chloride in a nitrogen atmosphere. All solid reagents and reference compounds were checked for purity by GLC. Some of these were recrystallized before use.

**Procedure.** Phenyl radicals were generated from $PhN_2^+BF_4^-$ by reduction with $Bu_4N^+I^-$ in dichloromethane. A solution of the aromatic hydrocarbon and $PhN_2^+BF_4^-$ in dichloromethane was allowed to come to thermal equilibrium at 298 K under a nitrogen atmosphere before an excess of a solution of $Bu_4N^+I^-$ was injected in the same solvent. The very rapid reaction was allowed to go to completion with efficient stirring and then allowed to stand for 0.5 h. The reaction mixture was then treated with 10% $Na_2S_2O_3$ solution to destroy iodine and extracted with pentane. The combined extracts were dried over anhydrous $MgSO_4$ before GLC analysis. The analysis was carried out with a Varian 3700 gas chromatograph in conjunction with a Hewlett-Packard 3390 A integrator. GLC response factors were determined by measurements on mixtures of known composition. All other aspects of the analysis were similar to those described earlier.[22]

**Acknowledgment.** This research was supported by the National Science Foundation (Grant CHE-8803480) and the donors of the Petroleum Research Fund, administered by the American Chemical Society.

**Registry** No. Benzene, 71-43-2; naphthalene, 91-20-3; anthracene, 120-12-7; pyrene, 129-00-0; chrysene, 218-01-9; triphenylene, 217-59-4; 1,2-benzanthracene, 56-55-3; phenanthracene, 85-01-8; phenyl radical, 2396-01-2.

(28) *Vogel's Textbook of Practical Organic Chemistry*; Longman: Harlow, Essex, U.K., 1978; p 705.

(29) Kobayoshi, T.; Nagokura, S. *J. Chem. Soc. Jpn.* **1974**, *47*, 2563.

(30) Klessinger, M. *Angew. Chem., Int. Ed. Engl.* **1972**, *11*, 525.

# Chelation of 2-Substituted-1-lithoxides: Structural and Energetic Factors of Relevance to Synthetic Organic Chemistry

**Michael A. Nichols, Andrew T. McPhail, and Edward M. Arnett***

*Contribution from the Department of Chemistry, Duke University, Durham, North Carolina 27706.* *Received February 5, 1991*

**Abstract:** A number of lithium 2-(methylamino)-, 2-(dimethylamino)-, 2-methoxy-, and 2-(isopropylthio)-substituted-1-phenyl-1-propoxides were studied as models for asymmetric synthetic strategies for which lithium chelation between two electronegative atoms has frequently been invoked. The heats of formation of these alkoxides were determined by deprotonating the alcohols with lithium bis(trimethylsilyl)amide in a solution calorimeter. Aggregation numbers for the substituted alcohols and their corresponding lithium alkoxides were obtained with freezing point depression and vapor pressure osmometry in THF, benzene, and dioxane. In several cases, solution structures were obtained through $^1H$, $^6Li$, and 2D $^6Li$-$^1H$ NOE (HOESY) NMR spectroscopy. Solid-state structures of lithium (+)-*N*-methylpseudoephedrate and (−)-*N*-methylephedrate (+)-*N*-methylpseudoephedrate and (−)-*N*-methylephedrate (as the benzene solvate) were obtained by X-ray crystallography, and both were found to be present as tetramers in which the dimethylamino nitrogen atoms were coordinated to the lithium cations to form five-membered chelate rings. The lithium alkoxides were either tetramers or hexamers in nonpolar solvents; however, the alkoxides' solution structures were very complex in THF as evidenced by several $^6Li$ resonances observed in the $^6Li$ NMR spectra at low temperatures. Intramolecular lithium chelation was found to occur in each alkoxide in dioxane and benzene. The enthalpies of chelational stabilization were estimated by comparing their heats of deprotonation with those of nonchelatable 2-alkyl-substituted analogues. The stabilization enthalpies ranged from 5 to 11 kcal/mol per alkoxide molecule.

## Introduction

Important progress toward asymmetric synthesis has been made in the last two decades through the use of organolithium compounds in low polarity solvents, usually at low temperatures. Especially successful has been the use of lithium enolates in the modern aldol reaction.[1,2] Although the actual reactive inter-

0002-7863/91/1513-6222$02.50/0 

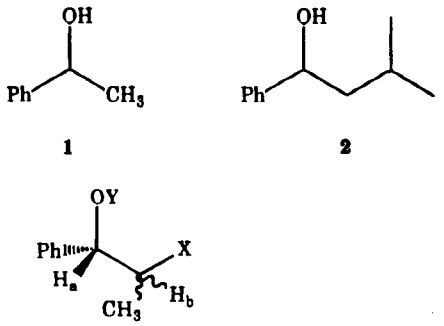


3: X = $CH_3$
4: X = $CH_2CH_3$*
5: X = $NHCH_3$(1S,2S)-anti, Y = H;
5a: Y = Li
6: X = $NHCH_3$(1R,2S)-syn, Y = H;
6a: Y = Li
7: X = $N(CH_3)_2$(1S,2S)-anti, Y = H;
7a: Y = Li
8: X = $N(CH_3)_2$(1R,2S)-syn, Y = H;
8a: Y = Li
9: X = $OCH_3$**, Y = H;
9a: Y = Li
10: X = $SCH(CH_3)_2$***, Y = H;
10a: Y = Li

**Figure 1.** The 2-substituted-1-phenyl-1-propanols used in these studies. The anti and syn designations refer to the relative stereochemistry between the 1-phenyl and 2-methyl groups when the hydroxyl and X groups are drawn as shown above: (*) a 55:45 mixture of ±-(1*R*,2*R*)/(1*R*,2*S*) diastereomers was used; (**) an 87:13 mixture of the (±)-(1*R*,2*S*)-syn/(±)-(1*R*,2*R*)-anti diastereomers was used; (***) an 88:12 mixture of the (±)-(1*R*,2*R*)-anti/(±)-(1*R*,2*S*)-syn diastereomers was used.

mediate leading to the transition structure of the aldol reaction is not yet settled,[1a-c,3,4] chelation of lithium between the β-situated carbonyl and alkoxide moieties is a common feature in all proposed transition structures and is now thoroughly underwritten by structure determination of the lithium aldolate both in the crystal structure[5] and in solution.[6]

Although the exact nature of the "lithium bond" between two electronegative atoms is somewhat controversial[7] and is clearly differentiated from the hydrogen bond, the high charge density of the lithium ion and the stereospecificity obtained in the aldol reaction under the conditions where chelation should be optimal have convinced most workers in the field that lithium chelation plays a deciding role in the modern aldol reaction.[8]

Solution[9] and X-ray[9a,10] structures obtained in recent years demonstrate unequivocally the powerful role of lithium ion in assembling anionic units into ion pairs, ion triplets, dimers, tetramers, hexamers, and higher aggregates. Thermochemical estimates of chelation energy for a variety of proximally substituted aryl- and alkyllithium compounds have been reported by Beak[11] and Klumpp,[12] while Houk and Schleyer[13] have examined theoretical structures and energy components. Several X-ray structures of intramolecularly chelated organolithium compounds have been reported during the past decade.[12,14-16]

In addition to the variants of the aldol addition of lithium enolates to carbonyl groups, other strategies for asymmetric synthesis have been employed with chiral oxazolines,[17] chiral hydrazones,[18] and chiral imide enolates.[1a-c] Lithium chelation has also been implicated as an important feature of Beak's "dipole-stabilized carbanions".[19] Again, a key feature in the interpretation of these stereoselective processes is chelation of lithium between two suitably positioned electronegative elements, usually either oxygen or nitrogen. However, there are relatively few direct experimental, structural,[14-16] or thermodynamic data[11,12] which demonstrate the presence of lithium chelation or evaluate its strength under conditions comparable to those used for synthesis.

This article reports experiments designed to address such data through comparison of the heats of formation of a variety of 2-substituted-1-lithoxide ions and comparison of their structures

(1) For reviews of the modern aldol reaction, see: (a) Heathcock, C. H. In *Asymmetric Synthesis*; Morrison, J. D., Ed.; Academic Press: New York, 1984; Vol. 3, Part B, Chapter 2. (b) Evans, D. A. In *Asymmetric Synthesis*; Vol. 3, Part B, Chapter 1. (c) Evans, D. A.; Nelson, J. V.; Taber, T. R. In *Topics in Stereochemistry*; Allinger, N. L., Eliel, E. L., Wilen, S. H., Eds.; Wiley: New York, 1982; Vol. 13, pp 1-115. (d) Hajos, Z. G. In *Carbon-Carbon Bond Formation*; Augustine, R. L., Ed.; Marcel Dekker: New York, 1979; Vol. 1, Chapter 1.

(2) The use of organomagnesium reagents predates the "modern aldol reaction", see: (a) Neilson, A. T.; Houlihan, W. J. *Org. React.* **1968**, *16*, 1-403. (b) Neilson, A. T.; Gibbons, C.; Zimmerman, C. A. *J. Am. Chem. Soc.* **1951**, *73*, 4696.

(3) Zimmerman, H.; Traxler, M. *J. Am. Chem. Soc.* **1957**, *79*, 1920.

(4) Aggregated aldol transition states have been proposed in the following: (a) Seebach, D.; Amstutz, R.; Dunitz, J. D. *Helv. Chim. Acta* **1981**, *64*, 2622. (b) Heathcock, C. H.; Lampe, J. *J. Org. Chem.* **1983**, *48*, 4330. (c) Williard, P. G.; Hintze, M. J. *J. Am. Chem. Soc.* **1987**, *109*, 5539-5541.

(5) Williard, P. G.; Salvino, J. M. *Tetrahedron Lett.* **1985**, *26*, 3931-3934.

(6) Arnett, E. M.; Fisher, F. J.; Nichols, M. A.; Ribeiro, A. A. *J. Am. Chem. Soc.* **1990**, *112*, 801-808.

(7) Sannigrahi, A. B.; Kar, T.; Niyogi, B. G.; Hobza, P.; Schleyer, P. v. R. *Chem. Rev.* **1990**, *90*, 1061-1076, and references therein.

(8) See, however: Das, G.; Thorton, E. R. *J. Am. Chem. Soc.* **1990**, *112*, 5360-5362.

(9) Leading references for organolithium solution structures can be found: (a) Seebach, D. *Angew. Chem., Int. Ed. Engl.* **1988**, *27*, 1624-1654. (b) Wakefield, B. J. *The Chemistry of Organolithium Compounds*; Pergamon: New York, 1974. (c) Jackman, L. M.; Lange, B. C. *Tetrahedron* **1977**, *33*, 2737-2769.

(10) Reviews of organolithium X-ray structures: (a) Setzer, W. N.; Schleyer, P. v. R. *Adv. Organomet. Chem.* **1985**, *24*, 354-450. (b) Seebach, D. In *Proceedings of the Robert A. Welch Foundation Conferences on Chemistry and Biochemistry*; Wiley: New York, 1984; p 93. (c) Reference 9a.

(11) Beak, P.; Siegal, B. *J. Am. Chem. Soc.* **1974**, *96*, 6803-6805.

(12) For leading references, see: Klumpp, G. W. *Recl. Trav. Chim. Pays-Bas* **1986**, *105*, 1-21.

(13) (a) Rondan, N. G.; Houk, K. N.; Beak, P.; Zajdel, W. J.; Chandrasekhar, J.; Schleyer, P. v. R. *J. Org. Chem.* **1981**, *46*, 4108-4110. (b) Clark, T.; Schleyer, P. v. R.; Houk, K. N.; Rondan, N. G. *J. Chem. Soc., Chem. Commun.* **1981**, 579-581. (c) Schleyer, P. v. R.; Andrade, J. These values were reported in ref 12.

(14) (a) Moene, W.; Schakel, M.; Hoogland, G. J. M.; de Kanter, F. J. J.; Klumpp, G. W.; Spek, A. L. *Tetrahedron Lett.* **1990**, *31*, 2641-2642. (b) Dietrich, H.; Mahdi, W.; Storck, W. *J. Organomet. Chem.* **1988**, *349*, 1-10. (c) Harder, S.; Boersma, J.; Brandsma, L.; van Heteren, A.; Kanters, J. A.; Bauer, W.; Schleyer, P. v. R. *J. Am. Chem. Soc.* **1988**, *110*, 7802-7806. (d) Jastrzebski, J. T. B. H.; van Koten, G.; Konijn, M.; Stam, C. H. *J. Am. Chem. Soc.* **1982**, *104*, 5490-5492. (e) Bauer, W.; Klusener, P. A. A.; Harder, S.; Kanters, J. A.; Duisenberg, A. J. M.; Brandsma, L.; Schleyer, P. v. R. *Organometallics* **1988**, *7*, 552-555. (f) Harder, S.; Boersma, J.; Brandsma, L.; Kanters, J. A.; Bauer, W.; Schleyer, P. v. R. *Organometallics* **1989**, *8*, 1696-1700. (g) Klumpp, G. W.; Geurink, P. J. A.; Spek, A. L.; Duisenberg, A. J. M. *J. Chem. Soc., Chem. Commun.* **1983**, 814-816. (h) Speck, A. L.; Duisenberg, A. J. M.; Klumpp, G. W.; Geurink, P. J. A. *Acta Crystallogr.* **1984**, *C40*, 372-374. (i) Jastrzebski, J. T. B. H.; van Koten, G.; Goubitz, K.; Arlen, C.; Pfeffer, M. *J. Organomet. Chem.* **1983**, *246*, C75-C79. (j) Klumpp, G. W.; Geurink, P. J. A.; van Eikema Hommes, N. J. R.; de Kanter, F. J. J.; Vos, M.; Spek, A. L. *Recl. Trav. Chim. Pays-Bas* **1986**, *105*, 398-403. (k) Klumpp, G. W.; Vos, M.; de Kanter, F. J. J. *J. Am. Chem. Soc.* **1985**, *107*, 8292-8294. (l) Lee, K. S.; Williard, P. G.; Suggs, J. W. *J. Organomet. Chem.* **1986**, *299*, 311-317. (m) Moene, W.; Vos, M.; de Kanter, F. J. J.; Klumpp, G. W.; Spek, A. L. *J. Am. Chem. Soc.* **1989**, *111*, 3463-3465. (n) Vos, M.; de Kanter, F. J. J.; Schakel, M.; van Eikema Hommes, N. J. R.; Klumpp, G. W. *J. Am. Chem. Soc.* **1987**, *109*, 2187-2188. (o) Polt, R. L.; Stork, G. L.; Carpenter, G. B.; Williard, P. G. *J. Am. Chem. Soc.* **1984**, *106*, 4276-4277.

(15) (a) Wanat, R. A.; Collum, D. B.; Van Duyne, G.; Clardy, J.; DePue, R. T. *J. Am. Chem. Soc.* **1986**, *108*, 3415-3422. (b) Enders, D.; Bachstadtler, G.; Kremer, K. A.; Marsch, M.; Harms, K.; Boche, G. *Angew. Chem., Int. Ed. Engl.* **1988**, *27*, 1522-1523. (c) Jastrzebski, J. T. B. H.; van Koten, G.; Christophersen, M. J. N.; Stam, C. H. *J. Organomet. Chem.* **1985**, *292*, 319-324. (d) Jastrzebski, J. T. B. H.; van Koten, G.; van de Mieroup, W. F. *Inorg. Chim. Acta* **1988**, *142*, 169-171. (e) Maetzke, T.; Pirmin Hidber, C.; Seebach, D. *J. Am. Chem. Soc.* **1990**, *112*, 8248-8250. (f) Ahlbrecht, H.; Boche, G.; Harms, K.; Marsch, M.; Sommer, H. *Chem. Ber.* **1990**, *123*, 1853-1858.

(16) Arnett, E. M.; Nichols, M. A.; McPhail, A. T. *J. Am. Chem. Soc.* **1990**, *112*, 7059-7060.

(17) (a) For leading references, see: Meyers, A. I. In *Asymmetric Synthesis*; Morrison, J. D., Ed.; Academic Press: New York, 1984; Vol. 3, Part B, pp 213-274. (b) Meyers, A. I. *Aldrich. Acta* **1985**, *18*, 59-68.

(18) Enders, D. In *Asymmetric Synthesis*; Morrison, J. D., Ed.; Academic Press: New York, 1984; Vol. 3, Part B, pp 275-339.

(19) For leading references, see: Beak, P.; Zajdel, W. J. *Chem. Rev.* **1984**, *84*, 471-523.

in nonpolar solvents. The heats of deprotonation of a series of β-substituted alcohols (Figure 1) with alkali bis(trimethylsilyl)-amides in several nonpolar solvents were determined through calorimetric titration of the initial alcohol. Aggregation numbers for the substituted alcohols and their corresponding lithium alkoxides were obtained with freezing point depression and vapor pressure osmometry. In several cases, solution structures were obtained through $^1H$ and $^6Li$ NMR and 2D $^6Li$-$^1H$ NOE (HOESY) NMR spectroscopy.

Particular emphasis was given to two diastereomeric chiral β-amino alcohols, pseudoephedrine (**5**) and ephedrine (**6**), by virtue of their relevance to model transition structures for asymmetric synthesis.[17,18] Suitable crystals of the lithium salts of (+)-*N*-methylpseudoephedrine[16] (**7**) and (−)-*N*-methylephedrine (**8**) could be isolated, and their structures were determined by X-ray crystallography.

## Experimental Section

**Materials and General Procedures.** All compounds whose purification is not mentioned explicitly in this section were purified by standard techniques.[20] Purity was checked by $^1H$ NMR, melting point, and boiling point, where applicable. Tetrahydrofuran (Fisher) and benzene (Mallinckrodt) were distilled from the sodium/benzophenone ketyl. *p*-Dioxane (Aldrich) was refluxed over sodium metal until the metal surface remained clean and was distilled prior to use. The deuterated solvents were used directly from their commercial ampules. All manipulations were carried out under argon with standard techniques[21] or in a Vacuum Atmospheres drybox equipped with a VAC HE-493 purification system. Proton and $^{13}C$ NMR spectra were recorded with a General Electric QE-300 NMR spectrometer at ambient temperatures. Chemical shifts are reported relative to the residual carbons or protons of the solvent.

**Purification of the Alkali Bis(trimethylsilyl)amide Bases.** Lithium bis(trimethylsilyl)amide (LHMDS, Aldrich) was purified by sublimation and stored in a drybox under vacuum in a Schlenk flask. [$^6$Li]HMDS was prepared as described previously[6] and stored under vacuum. Solid sodium bis(trimethylsilyl)amide (NaHMDS, 1.0 M solution in THF, Aldrich) was isolated by removing the solvent in vacuo and was recrystallized from pentane at −80 °C. The solid was dried under vacuum, 0.1 Torr for 24 h. Potassium bis(trimethylsilyl)amide (KHMDS, Callery Chemical Co.) was recrystallized from toluene at −80 °C. Toluene was removed from the complex[22] under vacuum, 0.10 Torr for 48 h.

**General Purification of the Alcohols.** All the alcohols employed in this study were purified either by sublimation or vacuum distillation and stored under argon in a drybox prior to use. (−)-Ephedrine (**6**), (−)-*N*-methylephedrine (**8**), (+)-pseudoephedrine (**5**), and (+)-*N*-methylpseudoephedrine (**7**) (all from Aldrich) were purified by sublimation and stored in a drybox under vacuum in a Schlenk flask prior to use. *sec*-Phenethanol (**1**) (Aldrich) was dried with sodium metal and distilled under vacuum, bp 60 °C at 3 Torr. 2-Methyl-1-phenyl-1-propanol (**3**) was prepared by the reduction of isobutyrophenone (Aldrich) with $LiAlH_4$ in THF at 0 °C and purified by vacuum distillation, bp 60 °C at 0.8 Torr. 3-Methyl-1-phenyl-1-butanol (**2**) was prepared by the addition of isovaleraldehyde (Aldrich) to phenyl magnesium bromide in THF at 0 °C, followed by refluxing for 1 h. The alcohol was purified by vacuum distillation, bp 85–86 °C at 0.8 Torr.

**Synthesis of 2-Methoxy-1-phenyl-1-propanol (9).** This alcohol was prepared by the addition of 2-methoxypropiophenone[23] to a suspension of $LiAlH_4$ (Fluka, 95%) in THF at 0 °C. The solution was stirred an additional 12 h, and the crude product was purified by column chromatography and vacuum distillation, bp 92–94 °C at 0.5 Torr, yielding a colorless oil. The purified yield was 90%. An 87:13 mixture of the syn/anti diastereomers was determined with use of $^1H$ NMR integration with the stereochemistry of the major diastereomer assigned based upon literature precedent.[24]

**(±)-Syn Diastereomer.** $^1H$ NMR (300.1 MHz, $CHCl_3$-*d*) δ 7.4–7.2 (m, Ar-H, 5 H), 4.89 (d, *J* = 3.5 Hz, ArCH–, 1 H), 3.52 (dq, *J* = 3.3, 6.3 Hz, –CH(OMe)–, 1 H), 3.40 (s, $-OCH_3$, 3 H), 2.55 (br, –OH, 1 H), 0.96 (d, *J* = 6.5 Hz, $-CH_3$, 3 H); $^{13}C(^1H)$ NMR (75.5 MHz, $CHCl_3$-*d*) δ 140.3 (ipso-ArC), 127.9 (ArC), 127.1 (ArC), 126.0 (ArC), 80.5 (PhCH(OH)–), 74.2 (–CH(OMe)–), 56.4 ($-OCH_3$), 12.4 ($-CH_3$).

**(±)-Anti Diastereomer.** $^1H$ NMR (300.1 MHz, $CHCl_3$-*d*) δ 7.4–7.2 (m, Ar-H, 5 H), 4.30 (d, *J* = 7.9 Hz, ArCH–, 1 H), 3.52 (dq, *J* = 3.3, 6.3 Hz, –CH(OMe)–, 1 H), 3.40 (s, $-OCH_3$, 3 H), 2.55 (br, –OH, 1 H), 0.96 (d, *J* = 6.5 Hz, $-CH_3$, 3 H); $^{13}C(^1H)$ NMR (75.5 MHz, $CHCl_3$-*d*) δ 140.3 (ipso-ArC), 127.9 (ArC), 127.1 (ArC), 126.0 (ArC), 81.7 (PhCH(OH)–), 78.2 (–CH(OMe)–), 56.4 ($-OCH_3$), 14.7 ($-CH_3$); IR (neat, ZnS plates) 3436, 3030–3060, 2825–2980, 1708, 1452 $cm^{-1}$. C, H Anal. Theoretical: C, 72.29; H, 8.43. Found: C, 72.30; H, 8.44.

**Synthesis of 2-(Isopropylthio)-1-phenyl-1-propanol (10).** 2-(Isopropylthio)-1-phenyl-1-propanone[25] was added to $LiAlH_4$ (0.5 equiv) in THF at 0 °C and stirred an additional 12 h at 25 °C. The product was purified by column chromatography and vacuum distillation, bp 135 °C at 3 Torr. The final purified yield was 88%. $^1H$ NMR integration indicated that the product contained an 88:12 mixture of the anti/syn diastereomers. The stereochemistry of the major diastereomer was determined by converting the alcohol to the epoxide via alkylation with $Me_3OBF_4$ and deprotonation with NaOH.[26] An 87:13 ratio of *cis*/*trans*-2-methyl-3-phenyloxirane was obtained, confirming the major diastereomer to be the anti compound.

**(±)-Anti Isomer.** $^1H$ NMR (300.1 MHz, $CHCl_3$-*d*, Eu(HFC)$_3$) δ 7.4–7.2 (m, Ar-H, 5 H), 4.27 (d, *J* = 8.5 Hz, –CH(OH)–, 1 H), 2.87 (m, –SC*H*$(CH_3)_2$, –C*H*S(*i*-Pr), 2 H), 1.22 (d, *J* = 6.5 Hz, –SCH(C*H*$_3)_2$, 3 H), 1.20 (d, *J* = 6.5 Hz, –SCH(C*H*$_3)_2$, 3 H), 1.09 (d, *J* = 7.0 Hz, $-CH_3$, 3 H); $^{13}C(^1H)$ NMR (75.5 MHz, $CHCl_3$-*d*, Eu(HFC)$_3$) δ 141.6 (ipso-ArC), 128.3 (ArC), 126.9 (ArC), 77.5 (–*C*H(OH)–), 49.2 (–S*C*H$(CH_3)_2$), 35.5 (–*C*HS(*i*-Pr)–), 24.4 (–SCH(*C*H$_3)_2$), 24.1 (–SCH(*C*H$_3)_2$), 19.8 ($-CH_3$).

**(±)-Syn Isomer.** $^1H$ NMR (300.1 MHz, $CHCl_3$-*d*, Eu(HFC)$_3$) δ 7.4–7.2 (m, Ar-H, 5 H), 4.86 (d, *J* = 4.59 Hz, –C*H*(OH)–, 1 H), 3.10 (m, –SC*H*$(CH_3)_2$, –C*H*S(*i*-Pr), 2 H), 1.33 (d, *J* = 6.5 Hz, –SCH(C*H*$_3)_2$, 3 H), 1.20 (d, *J* = 6.5 Hz, –SCH(C*H*$_3)_2$, 3 H), 1.04 (d, *J* = 7.0 Hz, $-CH_3$, 3 H); $^{13}C(^1H)$ NMR (75.5 MHz, $CHCl_3$-*d*, Eu(HFC)$_3$) δ 140.5 (ipso-ArC), 128.2 (ArC), 126.1 (ArC), 74.0 (–*C*H(OH)–), 46.3 (–S*C*H$(CH_3)_2$), 34.0 (–*C*HS(*i*-Pr)–), 24.4 (–SCH(*C*H$_3)_2$), 24.1 (–SCH(*C*H$_3)_2$), 14.6 ($-CH_3$); IR (neat, ZnS plates) 3424, 3030–3062, 2866–2965 $cm^{-1}$. C, H, S Anal. Theoretical: C, 68.57; H, 8.57; S, 15.24. Found: C, 68.72; H, 8.66; S, 14.97.

**Synthesis of 2-Methyl-1-phenyl-1-butanol (4).** 2-Methyl-1-phenyl-1-butanone was added to $LiAlH_4$ (0.5 equiv) in THF at 0 °C. The crude alcohol was purified by vacuum distillation, bp 78–79 °C at 0.8 Torr. The total purified yield was 78%. A 59:41 mixture of diastereomers was found by $^1H$ NMR integration, with the major diastereomer assigned as the (±)-(1*R*,2*R*) isomer based upon a literature precedent.[27]

**(±)-(1*R*,2*R*) Diastereomer.** $^1H$ NMR (300.1 MHz, $CHCl_3$-*d*) δ 7.4–7.2 (m, 5 H, ArH), 4.43 (d, *J* = 6.98 Hz, 1 H, PhC*H*(OH)–), 2.04 (br, 1 H, –OH), 1.75 (m, 1 H), PhCH(OH)C*H*–), 1.75 (m, 1 H, $-CH_2-$), 1.20 (m, 1 H, $-CH_2-$), 1.10 (m, 3 H, $-CH_2CH_3$), 0.75 (d, *J* = 6.79 Hz, 3 H, PhCH(OH)CH)C*H*$_3$)–); $^{13}C(^1H)$ NMR (75.5 MHz, $CHCl_3$-*d*) δ 143.5 (ipso-ArC), 128.1 (ArC), 127.3 (ArC), 126.7 (ArC), 78.8 (Ph*C*H(OH)–), 41.6 (PhCH(OH)*C*H–), 24.8 ($-CH_2-$), 15.0 (PhCH(OH)CH(*C*H$_3$)–), 11.3 ($-CH_2CH_3$).

**(±)-(1*R*,2*S*) Diastereomer.** $^1H$ NMR (300.1 MHz, $CHCl_3$-*d*) δ 7.4–7.2 (m, 5 H, ArH), 4.52 (d, *J* = 5.96 Hz, 1 H, PhCH(OH)C*H*–), 2.04 (br, 1 H, –OH), 1.75 (m, 1 H, PhCH(OH)C*H*–), 1.40 (m, 1 H, $-CH_2-$), 1.10 (m, 1 H, $-CH_2-$), 0.95 (m, 3 H, $-CH_2CH_3$), 0.95 (m, 3 H, PhCH(OH)CH(C*H*$_3$)–); $^{13}C(^1H)$ NMR (75.5 MHz, $CHCl_3$-*d*) δ 143.8 (ipso-ArC), 128.1 (ArC), 127.1 (ArC), 126.3 (ArC), 78.0 (Ph*C*H(OH)–), 41.9 (PhCH(OH)*C*H–), 25.8 ($-CH_2-$), 14.0 (PhCH(OH)CH(*C*H$_3$)–), 11.6 ($-CH_2CH_3$); IR (neat, ZnS plates) 3360, 3029–3063, 2869–2945 $cm^{-1}$. C, H Anal. Theoretical: C, 80.44; H, 9.82. Found: C, 80.21; H, 9.69.

**Molecular Mechanics Calculations.**[28] MM2 calculations were performed with Allinger's MM2(87) program,[29] which contained parameters to include intramolecular hydrogen-bonding contributions. These calculations were performed on a Digital Equipment Corporation VAX 8350 computer.

(20) Perrin, D. D.; Armarego, W. L. F.; Perrin, D. R. *Purification of Laboratory Chemicals*, 2nd ed.; Pergamon Press: New York, 1980.
(21) Shriver, D. F.; Drezdzon, M. A. *The Manipulation of Air-Sensitive Compounds*, 2nd ed.; Wiley: New York, 1986.
(22) Williard, P. G. *Acta Crystallogr.* **1988**, *C44*, 270–272.
(23) This compound was prepared by the addition of $AgNO_3$ to 2-bromopropiophenone in methanol: Giordano, C.; Castaldi, G.; Casagrande, F.; Abis, L. *Tetrahedron Lett.* **1982**, *23*, 1385–1386.
(24) Koga, K.; Yomoda, S. *Chem. Pharm. Bull.* **1972**, *20*, 526–538.
(25) Prepared as described in ref 23 with isopropyl thiol.
(26) Shanklin, J. R.; Johnson, C. R.; Ollinger, J.; Coates, R. M. *J. Am. Chem. Soc.* **1973**, *95*, 3429–3430.
(27) Gonzalez, F. F.; Ossorio, R. P.; Plumet, J. *An. Quim.* **1975**, *71*, 208–212.
(28) (a) Burket, U.; Allinger, N. L. *Molecular Mechanics: ACS Monograph 177*; American Chemical Society: Washington, DC, 1982. (b) Clark, T. *A Handbook of Computational Chemistry*; Wiley: New York, 1985, Chapter 2.
(29) (a) Allinger, N. L. *J. Am. Chem. Soc.* **1977**, *99*, 8127; *J. Comput. Chem.* **1989**, *10*, 503. (b) *QPCE Bulletin* **1990**, *10*, 33.

**Table I.** $pK_a$'s of 2-Substituted-1-phenyl-1-propanols as Determined by the Bordwell Indicator Method in Dimethyl Sulfoxide at 25 °C[a]

| compound | $pK_a$ |
|---|---|
| (+)-pseudoephedrine (**5**) | 26.59 ± 0.10 |
| (−)-ephedrine (**6**) | 26.57 ± 0.09 |
| (+)-*N*-methylpseudoephedrine (**7**) | 27.26 ± 0.12 |
| (−)-*N*-methylephedrine (**8**) | 26.96 ± 0.10 |

[a] Errors are given at the 95% confidence limit.

**Table II.** MM2(87)-Calculated Minimized Total Steric Energies for 2-Substituted-1-phenyl-1-propanols in kcal/mol

| compound | minimized energy |
|---|---|
| Nonchelated Models | |
| *sec*-phenethanol (**1**) | −0.781 |
| 2-methyl-1-phenyl-1-propanol (**3**) | 0.392 |
| 2-methyl-1-phenyl-1-butanol (59:41, *RR*/*RS*) (**4**) | 3.180[a] |
| 3-methyl-1-phenyl-1-butanol (**2**) | 3.045 |
| Potentially Chelated Compounds | |
| pseudoephedrine (**5**) | 1.569 |
| ephedrine (**6**) | 2.299 |
| *N*-methylpseudoephedrine (**7**) | 8.408 |
| *N*-methylephedrine (**8**) | 9.384 |
| *syn*-2-methoxy-1-phenyl-1-propanol (**9**) | 7.137[b] |
| *anti*-2-(isopropylthio)-1-phenyl-1-propanol (**10**) | 5.626[b] |

[a] Calculated as the weighted average of $E_{min}$ for the diastereomeric mixture: $E_{min}$ (RR), 2.257 kcal/mol; $E_{min}$ (RS), 4.508 kcal/mol. [b] Calculated for only the diastereomer indicated.

**Colligative Property Measurements.** The vapor pressure osmometric and cryoscopic techniques have been described previously.[6] The lithium alkoxides were generated in situ by the deprotonation of the alcohol with LHMDS in the solvent of interest.

**Variable-Temperature $^6$Li NMR.** $^6$Li NMR spectra were obtained with a General Electric GN-500 NMR spectrometer operated at 73.6 MHz. The $^6$Li 90° pulse width was determined in the usual manner.[30] The temperature inside the probe was measured by a thermocouple and is accurate to ±0.5 °C. The samples were permitted to equilibrate for 5 min prior to acquisition. All $^6$Li chemical shifts are reported relative to an external [$^6$Li]Br/acetone-$d_6$ reference ($\delta$ = 0 ppm). The [$^6$Li] alkoxides were used in all experiments and were generated in situ with solid [$^6$Li]HMDS.

**2D $^6$Li–$^1$H NOE NMR.**[31] NMR spectra were recorded on a General Electric GN-500 spectrometer equipped with a broad-band 10 mm probe and a Nicolet 1280 computer. Our implementation of the experiment has been described earlier.[6] In these experiments, a [$^6$Li] alkoxide solution (3 mL) was placed into a 10-mm NMR tube and capped with a rubber septum. All NMR spectra were acquired with nonspinning samples.

**Calorimetry.** Heats of deprotonation were determined at 6, 13, or 25 °C with a Tronac 458 isoperibol solution calorimeter. The basic operation of the instrument has been described previously.[32] Heats of deprotonation ($\Delta H_{dep}$) were measured by titrating 2 mL of a 0.1–0.2 M alcohol solution into 50 mL of a 0.1 M LHMDS solution in the solvent of interest. $\Delta H_{dep}$ values were calculated (in kcal/mol) by the standard method.[32]

**$pK_a$ Measurements in Dimethyl Sulfoxide ($Me_2SO$).** The $pK_a$ values of the ephedrine alcohols were measured in $Me_2SO$ at 25 °C with the Bordwell indicator method. This technique has been described in detail elsewhere.[33] Iminostilbene ($pK_a$ = 27.1) was used as the indicator in all measurements. $Me_2SO$ was purified by a method previously employed in this group.[33c] No ion-pairing or homohydrogen-bonding corrections were needed in any measurements.

**Table III.** Vicinal Coupling Constants ($^3J$, in Hz) for 2-Substituted-1-phenyl-1-propanols in Various Solvents

| compound | $^3J$ THF | $^3J$ benzene | $^3J$ dioxane | MM2(87) calcd $^3J$[a] |
|---|---|---|---|---|
| pseudoephedrine (**5**) | 7.9 | 8.0 | 7.9 | 12.96 (176.7) |
| ephedrine (**6**) | 4.0 | 3.8 | 4.0 | 3.89 (60.8) |
| *N*-methylpseudoephedrine (**7**) | 9.5 | 9.5 | 9.6 | 12.94 (175.7) |
| *N*-methylephedrine (**8**) | 4.4 | 3.6 | 4.4 | 4.73 (54.9) |
| *syn*-2-methoxy-1-phenyl-1-propanol (**9**)[b] | 4.4 | 3.8 | 4.4 | 4.44 (56.9) |
| *anti*-2-(isopropylthio)-1-phenyl-1-propanol (**10**)[b] | 5.8 | 7.8 | 6.3 | 13.00 (179.0) |

[a] Estimated from the dihedral angle (given in parentheses) between $H_a$ and $H_b$ (Figure 1) of the MM2(87)-optimized structure with the simplified Karplus equation.[36] [b] Couplings listed are for the major diastereomer only.

**Table IV.** VPO and Cryoscopic Aggregation Numbers ($n$) for 2-Substituted-1-phenyl-1-propanols in THF, Benzene, and Dioxane[c]

| compound | THF[a] | benzene[a] | dioxane[a] |
|---|---|---|---|
| *sec*-phenethanol (**3**) | 1.06 ± 0.12 (0.97 ± 0.10) | 1.07 ± 0.10 (1.00 ± 0.04) | 1.66 ± 0.22 (1.07 ± 0.09) |
| pseudoephedrine (**5**) | 1.00 ± 0.12 *b* | 1.00 ± 0.10 (1.04 ± 0.04) | 1.07 ± 0.15 *b* |
| ephedrine (**6**) | 1.05 ± 0.07 | 1.05 ± 0.40 (1.00 ± 0.10) | 1.07 ± 0.11 *b* |
| *N*-methylpseudoephedrine (**7**) | 1.00 ± 0.04 | 0.98 ± 0.08 (1.04 ± 0.07) | 0.97 ± 0.08 (0.91 ± 0.07) |
| *N*-methylephedrine (**8**) | 1.01 ± 0.06 | 1.02 ± 0.08 (1.02 ± 0.08) | 1.02 ± 0.09 (1.16 ± 0.11) |
| 2-methoxy-1-phenyl-1-propanol (**9**) | 0.95 ± 0.07 | 0.97 ± 0.07 (1.17 ± 0.12) | 1.03 ± 0.08 (0.97 ± 0.09) |
| 2-(isopropylthio)-1-phenyl-1-propanol (**10**) | 1.03 ± 0.09 | 0.90 ± 0.06 (0.82 ± 0.08) | 1.02 ± 0.10 (0.97 ± 0.09) |

[a] Concentrations were 0.1–0.2 M. [b] The lithium alkoxide precipitated from this solvent. [c] Cryoscopic results are given in parentheses.

## Results

**$pK_a$ Measurements in $Me_2SO$.** The acidities of the hydroxyl protons of the ephedrine alcohols were determined in $Me_2SO$ and are listed in Table I. As expected, all the ephedrine alcohols have approximately the same $pK_a$ in $Me_2SO$, ranging from 26.6 to 27.3 $pK_a$ units.

**MM2(87)-Calculated Energies of the Alcohols.** An important requirement for the thermochemical analysis to be discussed later is that the steric energies of the chelatable and nonchelatable alcohols must be similar. These energy terms were estimated using molecular mechanics calculations, with Allinger's MM2(87) program chosen since it included parameters for stabilizing contributions from intramolecular hydrogen bonding. Table II gives the minimized total steric energies ($E_{min}$) for the alcohols studied. The $E_{min}$ values for the nonchelatable alcohols range from −0.78 to 3.18 kcal/mol, while the chelatable alcohols have values ranging from 1.57 to 9.38 kcal/mol.

**Solution Conformations of the Alcohols.** It has been shown with IR spectroscopy that the ephedrine alcohols undergo intramolecular hydrogen bonding in solution.[34] The conformations of the ephedrine alcohols in solution have been determined by using $^1$H NMR[35] and examining the vicinal coupling constants ($^3J$) between $H_a$ and $H_b$ of **5–8**. (See Figure 1.) The vicinal coupling constant is related to the dihedral angle between $H_a$ and $H_b$ using a simplified form of the Karplus equation.[36] Table III lists the vicinal coupling constants for the chelatable alcohols determined

(30) Martin, M. L.; Martin, G. L.; Delpuech, J. J. *Practical NMR Spectroscopy*; Heyden: London, 1980; p 267.
(31) (a) Bauer, W.; Schleyer, P. v. R. *Magn. Reson. Chem.* **1988**, *26*, 827–833, and references therein. (b) Bauer, W.; Clark, T.; Schleyer, P. v. R. *J. Am. Chem. Soc.* **1987**, *109*, 970–977.
(32) Grime, J. K., Ed. *Analytical Solution Calorimetry*; Wiley: New York, 1985.
(33) (a) Matthews, W. S.; Bares, J. E.; Bartmess, J. E.; Bordwell, F. G.; Cornforth, F. J.; Drucker, G. E.; Margolin, Z.; McCallum, M. J.; McCollum, C. J.; Vanier, N. R. *J. Am. Chem. Soc.* **1975**, *97*, 7006. (b) Olmstead, W. N.; Bordwell, F. G. *J. Org. Chem.* **1980**, *45*, 3295, 3299. (c) Arnett, E. M.; Maroldo, S. G.; Schilling, S. L.; Harrelson, J. A. *J. Am. Chem. Soc.* **1984**, *106*, 6759–6767.
(34) Kanzawa, T. *Bull. Chem. Jpn. Soc.* **1956**, *29*, 398–403, 479–485, 604–608.
(35) Portoghese, P. S. *J. Med. Chem.* **1967**, *10*, 1057.
(36) (a) Karplus, M. *J. Chem. Phys.* **1959**, *30*, 11; *J. Am. Chem. Soc.* **1963**, *85*, 2870. (b) Bothner-By, A. A. *Adv. Magn. Reson.* **1965**, *1*, 195.

Table V. Combined VPO and Cryoscopic Aggregation Numbers for the Lithium 2-Substituted-1-phenyl-1-propoxides in THF, Benzene, and Dioxane[a]

| alkoxide | THF[b] | benzene[c] | dioxane[c] |
|---|---|---|---|
| *sec*-phenethanolate (1) | 4 | 4 | 6 |
| pseudoephedrate (5) | 6 | 4 | 6 |
| ephedrate (6) | 6[d] | 4, 6 | 6 |
| *N*-methylpseudoephedrate (7) | 4[d] | insoluble | 4 |
| *N*-methylephedrate (8) | 4[d] | 4 | 4 |
| 2-methoxy-1-phenyl-1-propanol (9) | 6[d] | 4, 6 | 4 |
| 2-(isopropylthio)-1-phenyl-1-propanol (10) | 6[d] | 4 | 4 |

[a] Concentrations were 0.1–0.2 M. [b] Multiple $^6$Li resonances were observed in the $^6$Li NMR spectra in THF-$d_8$. [c] Only one $^6$Li resonance was observed in the $^6$Li NMR spectra, whose chemical shift was invariant to temperature. [d] Only VPO results were obtained.

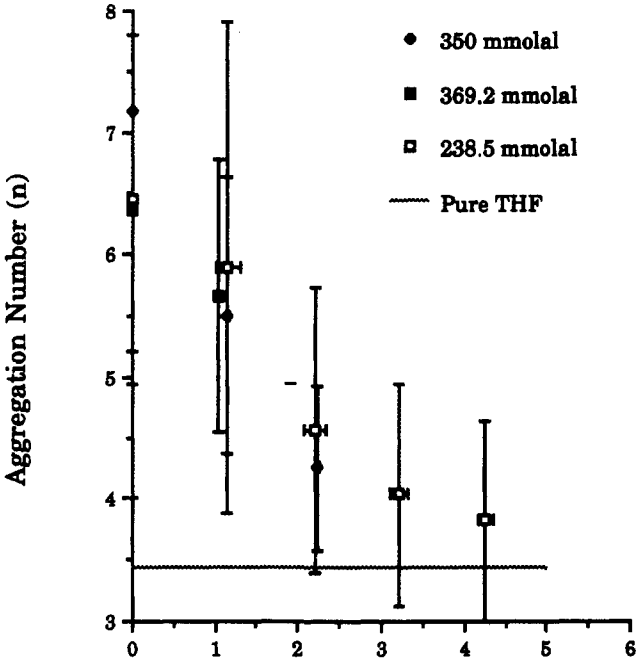


**Figure 2.** A VPO titration plot for lithium *sec*-phenethanolate in the presence of 1–4 equiv of THF in benzene (37 °C). The solid line on the plot corresponds to the aggregation number found in pure THF by VPO.

in THF, dioxane, and benzene. Also included are the calculated $^3J$ values from the optimized geometries that were determined with MM2(87). There is good agreement between the calculated and experimental $^3J$ values for those alcohols where the stereochemistry between the phenyl and 2-methyl protons is syn, but there is much poorer agreement for the anti alcohols. The differences translate into roughly a 30° difference in the dihedral angle between $H_a$ and $H_b$. The calculated and experimental conformations of all the chelatable alcohols indicated the presence of intramolecular hydrogen bonding.

**Solution Structures of the Lithium Alkoxides.** The aggregation states of the alcohols and their lithium alkoxides were determined with both VPO and cryoscopy in THF, dioxane, and benzene. These values are given in Tables IV and V, respectively. In all solvents, the alcohols were monomeric, whereas the alkoxides were either tetrameric or hexameric.

A VPO titration experiment was performed for the addition of THF to a benzene solution of lithium *sec*-phenethanolate. Evidence supporting the interaction of THF with this alkoxide is given in Figure 2, where the aggregation number of the alkoxide decreased as the amount of THF was increased.

Potential equilibria between aggregation states was probed with variable-temperature $^6$Li NMR. The $^6$Li NMR spectra for the [$^6$Li] alkoxides in THF-$d_8$ were quite complex, considerably

Table VI. Vicinal Coupling Constants ($^3J$, in Hz) for Lithium 2-Substituted-1-phenyl-1-propoxides in Benzene and Dioxane at 25 °C

| compound | benzene[a] | dioxane[a] |
|---|---|---|
| Li pseudoephedrate (5) | 8.3 | 8.4 |
| Li ephedrate (6) | 3.1 | 2.8 |
| Li *N*-methylpseudoephedrate (7) | 9.2 | insoluble |
| | 8.0 | 8.6 |
| Li *N*-methylephedrate (8) | *b* | 3.4 |
| Li *syn*-2-methoxy-1-phenyl-1-propoxide[c] (9) | *b* | *b* |
| Li *anti*-2-(isopropylthio)-1-phenyl-1-propoxide[c] (10) | 7.5 | 6.0 |
| | 6.8 | |

[a] Concentrations were 0.1–0.2 M. [b] The $^1$H spectra were not resolved sufficiently for $^3J$ to be determined. [c] Couplings listed are for the major diastereomer only.

Table VII. VPO and Cryoscopic Aggregation Numbers (*n*) for Lithium Bis(trimethylsilyl)amide (LHMDS) in Benzene (5.5, 37 °C), *p*-Dioxane (13, 37 °C), and THF (−108, 37 °C)

| solvent | *n* (VPO)[a] | *n* (cryoscopy)[a] |
|---|---|---|
| benzene | 2.31 ± 0.29 | 2.20 ± 0.52 |
| | | 2.14[b] |
| dioxane | 1.89 ± 0.23 | 2.20 ± 0.26 |
| THF | 1.17 ± 0.35 | 0.87 ± 0.03 |
| | 1.15, 1.03[b] | |

[a] Concentrations were 0.1–0.2 M. [b] From ref 37.

different, and sensitive to temperature variation. Figures 3 and 4, for the lithium salts of pseudoephedrine (5) and ephedrine (6) are typical of the series.

The variable-temperature $^6$Li NMR spectra for the lithium alkoxides in dioxane-$d_8$ and benzene-$d_6$ were also obtained and, in almost every case, only one $^6$Li resonance was observed, whose chemical shift was invariant to temperature. Thus, the $^6$Li spectra indicate that in THF either a variety of aggregated species exist in a temperature-dependent equilibrium or complex aggregates are formed at low temperatures. In benzene and dioxane, however, only one aggregate structure exists, where all the $^6$Li nuclei are magnetically equivalent.

The vicinal coupling constants ($^3J$) of the lithium alkoxides were measured in benzene and dioxane to gain more detailed information on the solution conformations. These are listed in Table VI. Three of the $^1$H NMR spectra were not sufficiently resolved to allow a $^3J$ value to be measured. There is very good agreement between the coupling constants measured for each alcohol/alkoxide pair in both solvents.

2D $^6$Li–$^1$H NOE NMR spectroscopy was also used to elucidate the detailed solution structures for the lithium alkoxides in benzene and dioxane. Figures 5 and 6 are the 2D $^6$Li–$^1$H NOE NMR spectra obtained for [$^6$Li] pseudoephedrate (**5a**) and ephedrate (**6a**) in dioxane-$d_8$ at 13 °C, respectively. The proton assignments for lithium pseudoephedrate and ephedrate were made with 2D $^1$H–$^1$H COSY and 2D $^1$H–$^{13}$C heteronuclear correlation NMR, respectively. In the case of lithium pseudoephedrate, a strong NOE crosspeak was observed from the amino proton to $^6$Li, indicating a short interatomic distance. (See Figure 5.)

**Solution Structures of LHMDS.** Since all the thermochemical experiments to be discussed later employed LHMDS as the base, its solution structures in THF, dioxane, and benzene were determined. Table VII lists the VPO and cryoscopic aggregation numbers determined in each solvent. The solution structures of LHMDS have been studied in benzene and THF by Brown and Kimura.[37] Excellent agreement was found between the previously determined aggregation numbers and the values obtained with our instruments. LHMDS is dimeric in benzene and dioxane[38] and has been shown to exist in a monomer–dimer equilibrium in THF.[37]

**Solid-State Structures.** Crystals of lithium (+)-*N*-methylpseudoephedrate[16] (**7a**) and (−)-*N*-methylephedrate (**8a**) were

(37) Brown, T. L.; Kimura, B. *J. Organomet. Chem.* **1971**, *26*, 57.

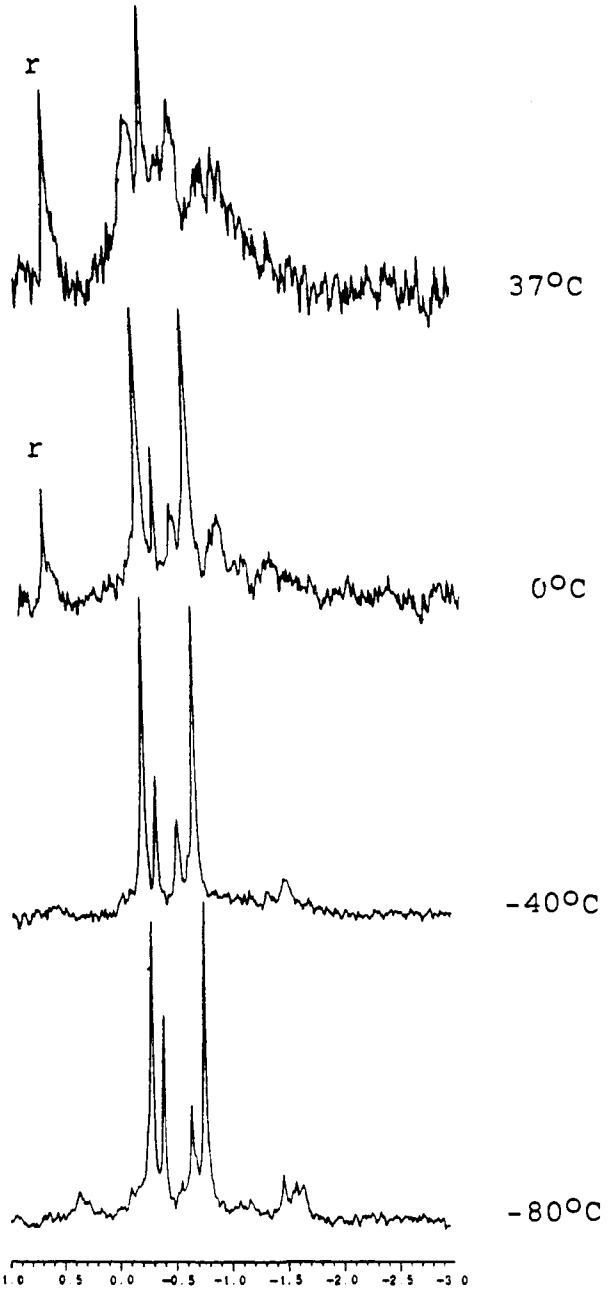


**Figure 3.** Variable-temperature $^6$Li NMR spectra for a 187.6 mM [$^6$Li](+)-pseudoephedrate (**5a**) solution in THF-$d_8$: *r* = reference signal, saturated [$^6$Li]Br in acetone-$d_6$. Line broadening of 1 Hz was applied to each $^6$Li spectrum.

obtained by precipitation from 95:5 dioxane/THF and benzene, respectively. The solid-state structures of these compounds were determined by X-ray crystallography, and an ORTEP diagram of the solid-state tetramer (**8a**)[39] is provided in Figure 7. The lithium cation clearly is chelated by the amino nitrogen in the tetrameric structure. Detailed crystallographic data have been submitted as supplementary material. An ORTEP diagram of the corresponding tetramer in crystals of lithium (+)-*N*-methylpseudoephedrate was published previously.[16]

**Calorimetry.** Heats of deprotonation ($\Delta H_{dep}$) of the 2-substituted-1-phenyl-1-propanols by LHMDS were determined calorimetrically by titrating an alcohol solution into an excess of the lithium amide base. The $\Delta H_{dep}$ values obtained in THF (25 °C), dioxane (13 °C), and benzene (6 °C) are listed in Tables VIII–X, respectively. In THF, $\Delta H_{dep}$ values were also determined with NaHMDS and KHMDS; however, the only significant trend that emerged from these data was that the deprotonation reaction with LHMDS was approximately 8 and 10 kcal/mol more exothermic than with NaHMDS and KHMDS, respectively. No consistent trends were observed when the alcohols were compared to each other with the same amide base. With LHMDS, the chelatable alcohols had similar $\Delta H_{dep}$ values (−19.1 to −21.8 kcal/mol), which were 8 kcal/mol more exothermic than the nonchelatable alcohols (−11.8 to −13.7 kcal/mol). *sec*-Phenethanol, a nonchelatable alcohol, did exhibit anomalous behavior as it had a $\Delta H_{dep}$ of −18.7 kcal/mol.

The $\Delta H_{dep}$ values measured in dioxane (Table IX, 13 °C) were similar to those obtained in THF; the heats of deprotonation of the chelatable alcohols were approximately 7–8 kcal/mol more exothermic than their nonchelatable analogues. *sec*-Phenethanol exhibited the same anomalous behavior in dioxane that was found in THF.

**Table VIII.** Heats of Deprotonation of 2-Substituted-1-phenyl-1-propanols with Alkali Disilylazide Bases in THF at 25 °C (in kcal/mol)[a]

| compound | $\Delta H_{deprotonation}$ using $M^+{}^-NTMS_2$ | | |
|---|---|---|---|
| | Li | Na | K |
| *sec*-phenethanol (**1**) | −18.7 ± 0.3 | −11.5 ± 0.2 | −6.8 ± 0.3 |
| 2-methyl-1-phenyl-1-propanol (**3**) | −13.7 ± 0.9 | | |
| 2-methyl-1-phenyl-1-butanol (**4**) | −11.8 ± 0.1 | | |
| 3-methyl-1-phenyl-1-butanol (**2**) | −12.2 ± 0.1 | | |
| pseudoephedrine (**5**) | −20.3 ± 0.4 | −12.1 ± 0.5 | −9.2 ± 0.1 |
| ephedrine (**6**) | −19.4 ± 0.3 | −13.5 ± 0.2 | −8.3 ± 0.2 |
| *N*-methylpseudoephedrine (**7**) | −19.1 ± 0.3 | −11.1 ± 0.3 | −7.0 ± 0.2 |
| *N*-methylephedrine (**8**) | −20.6 ± 0.2 | −14.6 ± 0.4 | −9.1 ± 0.1 |
| 2-(isopropylthio)-1-phenyl-1-propanol (**10**) | −21.8 ± 0.4 | | |

[a] Errors are given at the 95% confidence limit.

**Table IX.** Heats of Deprotonation of 2-Substituted-1-phenyl-1-propanols by LHMDS in Dioxane at 13 °C[a,b]

| compound | $\Delta H_{deprotonation}$ (kcal/mol) |
|---|---|
| Nonchelated Models | |
| *sec*-phenethanol (**1**) | −20.0 ± 0.9 |
| 2-methyl-1-phenyl-1-propanol (**3**) | −13.2 ± 0.3 |
| 2-methyl-1-phenyl-1-butanol (**4**) | −13.6 ± 0.3 |
| 3-methyl-1-phenyl-1-butanol (**2**) | −14.1 ± 0.8 |
| Potentially Chelated Compounds | |
| pseudoephedrine (**5**) | −20.5 ± 0.4 |
| ephedrine (**6**) | −21.8 ± 1.2 |
| *N*-methylpseudoephedrine (**7**) | insoluble |
| *N*-methylephedrine (**8**) | −20.5 ± 1.2 |
| 2-methoxy-1-phenyl-1-propanol (**9**) | −20.7 ± 0.2 |
| 2-(isopropylthio)-1-phenyl-1-propanol (**10**) | −18.8 ± 0.3 |

[a] Errors are given at the 95% confidence limit. [b] Corrected for the $\Delta H_{dilution}$ of HMDS into dioxane, +0.97 ± 0.10 kcal/mol.

**Table X.** Heats of Deprotonation of 2-Substituted-1-phenyl-1-propanols by LHMDS in Benzene at 6 °C[a,b]

| compound | $\Delta H_{deprotonation}$ (kcal/mol) |
|---|---|
| Nonchelated Models | |
| *sec*-phenethanol (**1**) | −26.6 ± 0.5 |
| 2-methyl-1-phenyl-1-propanol (**3**) | −26.2 ± 0.3 |
| 2-methyl-1-phenyl-1-butanol (**4**) | −27.2 ± 0.5 |
| 3-methyl-1-phenyl-1-butanol (**2**) | −27.6 ± 0.8 |
| Potentially Chelated Compounds | |
| pseudoephedrine (**5**) | −37.0 ± 1.0 |
| ephedrine (**6**) | −38.0 ± 1.0 |
| *N*-methylpseudoephedrine (**7**) | −33.0 ± 1.0 |
| *N*-methylephedrine (**8**) | −35.0 ± 1.0 |
| 2-methoxy-1-phenyl-1-propanol (**9**) | −33.0 ± 1.0 |
| 2-(isopropylthio)-1-phenyl-1-propanol (**10**) | −34.0 ± 1.0 |

[a] Errors are given at the 95% confidence limit. [b] Corrected for the $\Delta H_{dilution}$ of HMDS into benzene, +1.30 ± 0.10 kcal/mol.

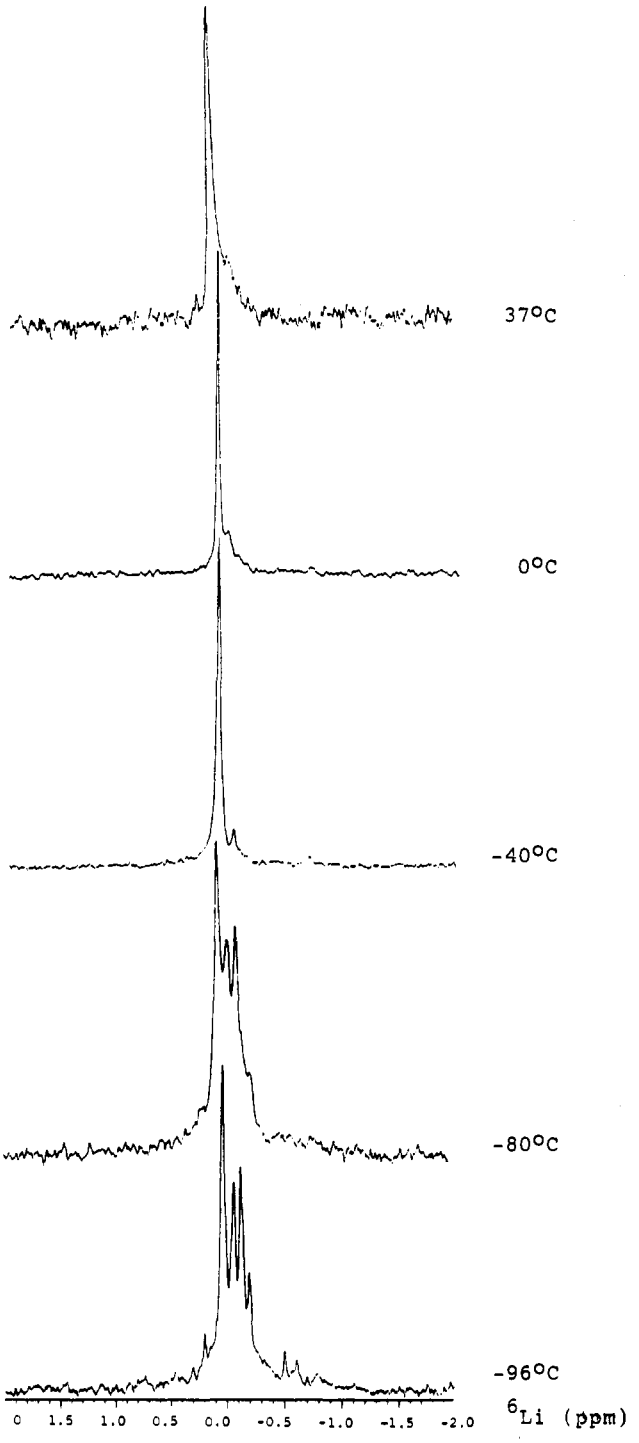


**Figure 4.** Variable-temperature $^6$Li NMR spectra for a 185.8 mM [$^6$Li](−)-ephedrate (**6a**) solution in THF-$d_8$. The NMR parameters are given on Figure 3. Line broadening of 1 Hz was applied to each $^6$Li spectrum.

The $\Delta H_{dep}$ values measured in benzene (Table X, 5 °C) were considerably more exothermic than in either THF or dioxane, with the chelatable alcohols having $\Delta H_{dep}$ ranging from −33.5 to −38.2 kcal/mol. These values were approximately 6–11 kcal/mol more exothermic than those obtained with the nonchelatable alcohols (−26.2 to −27.6 kcal/mol). In benzene, *sec*-phenethanol was found to have a $\Delta H_{dep}$ similar to the other nonchelatable alcohols.

## Discussion

The goal of the study presented here is to extend our previous investigations on the aldol reaction of lithium pinacolonate with pivalaldehyde in low polarity solvents[6] to the general question of the role that lithium chelation may play in a variety of other asymmetric synthetic strategies for which lithium chelation between two electronegative atoms has frequently been invoked.[1,17,18] A series of 2-substituted-1-phenyl-1-propanols was deprotonated with lithium, sodium, and potassium bis(trimethylsilyl)amide in several nonpolar solvents to provide heats of formation of the substituted alkali alkoxides.

Structural information concerning initial and final states of the thermochemical reactions was derived from vapor pressure osmometry and freezing point depression measurements to ascertain the states of aggregation. Several NMR techniques were used to obtain more detailed solution structure information about the 2-substituted-1-lithoxides. Fortunately, it was also possible to obtain suitable crystals for X-ray structural characterization of the lithium (+)-*N*-methylpseudoephedrate (**7a**) and (−)-*N*-methylephedrate (**8a**) diastereomers. As will be seen below, the results of these studies offer unequivocal evidence for lithium chelation between oxygen and nitrogen in the lithium β-amino alkoxides and a stabilization factor of 6–10 kcal/mol for these alkoxides and analogous methoxy- and 2-alkylthio alkoxides relative to nonchelatable alkyl-substituted analogues.

Although the results provide no direct evidence for the often proposed role of lithium chelation in the transition structures for asymmetric syntheses with oxazolines,[17] SAMP-hydrazones,[18] etc., they do demonstrate the reality of lithium chelation to electronegative atoms substituted at the β-position of aliphatic alkoxides and that this chelation involves a very significant stabilization factor.

**Solid-State Structure.** An ORTEP diagram of lithium (−)-*N*-methylephedrate is provided in Figure 7. The corresponding plot of the structure of lithium (+)-*N*-methylpseudoephedrate can be found in ref 16. Despite numerous attempts to obtain suitable crystals for the other lithoxides in this study, we were only successful in obtaining this diastereomeric pair.

Consistent with the structures of a wide variety of other proximally substituted lithium enolates[15c-e] and hydrazones,[15a,b] both of the compounds are tetrameric aggregates, and lithium chelation to the nearby amino nitrogen is apparent. Despite the clear overall similarity of the two chelated tetrameric arrangements, small differences in bond angles and torsional angles are observed. Lithium (−)-*N*-methylephedrate (**8a**) and (+)-*N*-methylpseudoephedrate (**7a**) are both present as discrete tetramers in the solid state. In crystals of the benzene solvate of **8a**, the shortest separation between the tetramers and benzene molecules at 3.74 Å involves a phenyl carbon atom and corresponds to a normal van der Waals type distance. As in other structures containing an $Li_4O_4$ core, this moiety may be viewed as consisting of four lithium atoms arranged in an approximately tetrahedral manner with an oxygen atom situated in the center of each of the $Li_3$ faces, thereby generating a distorted cube-like structure in which the diamond-shaped Li–O–Li–O faces (mean distances: Li···Li = 2.54 Å, O···O = 2.90 Å in **8a**; Li···Li = 2.53 Å, O···O = 2.93 Å in **7a**) are slightly puckered. Coordination of each of the lithium atoms is completed by the nitrogen atom of a chelating ligand to form five-membered Li–O–C–C–N rings (mean distances: Li–N = 2.12 Å, Li–O = 1.94 Å in **8a**; Li–N = 2.12 Å, Li–O = 1.93 Å in **7a**). In both **7a** and **8a**, an approximate $C_2$ symmetry axis passes through those pairs of cube faces ($Li_{123}$–$O_{14}$–$Li_{314}$–$O_{34}$, $Li_{234}$–$O_{24}$–$Li_{412}$–$O_{44}$) which share opposite edges with the five-membered rings. All of the five-membered rings in **7a** approximate to envelope forms with their methyl-bearing carbon center as the out-of-plane atom, and their C-methyl and phenyl substituents are both pseudoequatorially oriented. The syn configuration of the ligands in **8a** requires that adoption of a similar five-membered ring conformation means that either the C-methyl or phenyl ring substituent must occupy a pseudoaxial position, while the other must be pseudoequatorial. In **8a**, both of these alternative substituent dispositions are present, and small variations in the five-membered ring conformations are apparent in order to accommodate intramolecular interligand nonbonded substituent interactions. Two of the rings ($Li_{234}$–$O_{24}$–$C_{21}$–$C_{22}$–$N_{23}$, $Li_{314}$–$O_{34}$–$C_{31}$–$C_{32}$–$N_{33}$) adopt envelope conformations with their methyl-bearing carbon being the out-of-plane atom as in **7a**, one ($Li_{412}$–$O_{44}$–$C_{41}$–$C_{42}$–$N_{43}$) is in a half-chair conformation, while

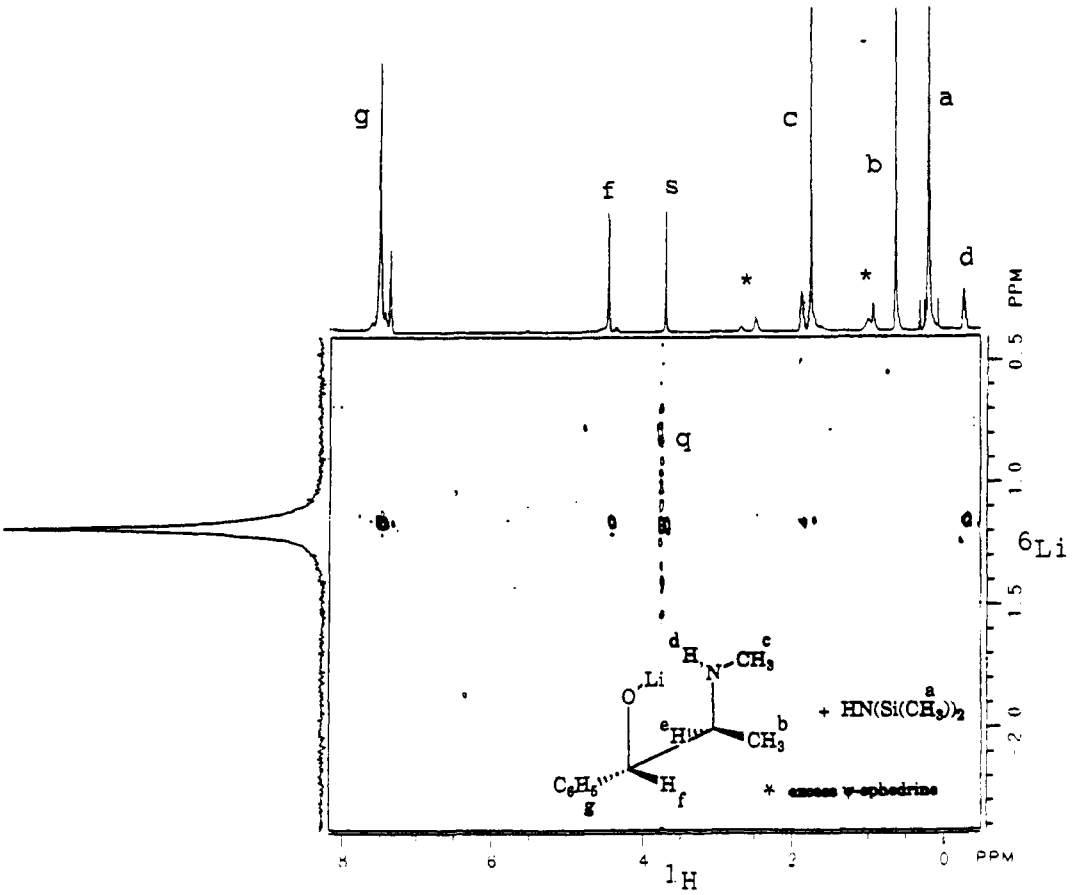


**Figure 5.** A 2D $^6$Li–$^1$H NOE NMR spectrum of a 200 mM [$^6$Li] (+)-pseudoephedrate (**5a**) solution in dioxane-$d_8$ at 13 °C: mixing time = 1.8 s, relaxation delay = 6 s, 256 increments in $t_1$, 16 scans acquired in $^6$Li per increment, 1K data points collected per scan, total acquisition time = 10.44 h. The $^6$Li resonance was referenced to external saturated LiOH/$D_2O$ ($\delta$ = 0 ppm): s = solvent, q = axial signal.

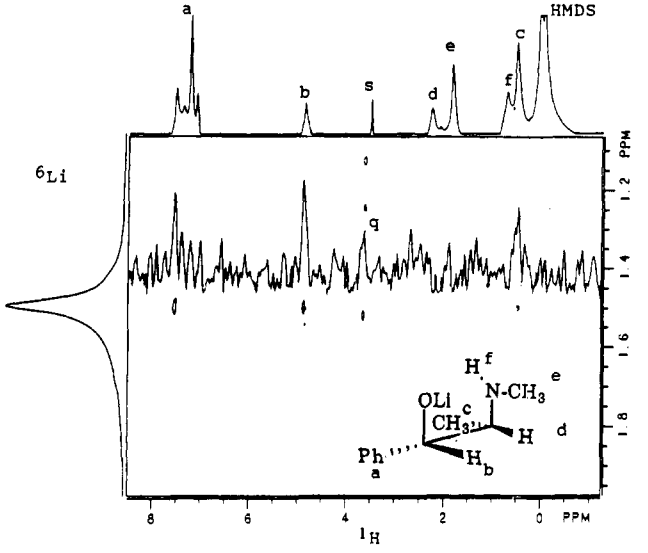


**Figure 6.** A 2D $^6$Li–$^1$H NOE NMR spectrum of a 250 mM [$^6$Li] (−)-ephedrate (**6a**) solution in dioxane-$d_8$ at 13 °C. NMR parameters are given in Figure 5. Insert: $f_1$ trace of the $^6$Li signal.

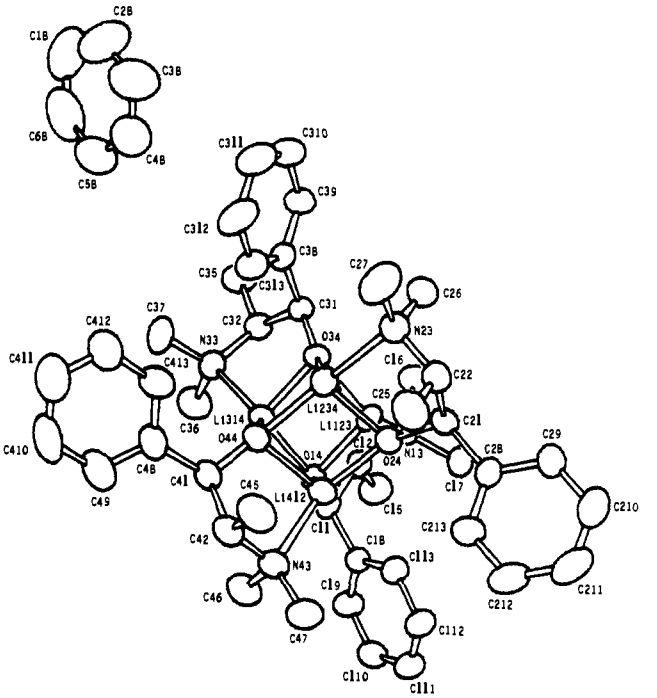

**Figure 7.** An ORTEP diagram (30% probability ellipsoids) of the structure of lithium (−)-*N*-methylephedrate (**8a**) in crystals of the benzene solvate. Hydrogen atoms have been omitted for clarity. The Li–O and Li–N bond distances range from 1.902 (9) to 1.972 (10) Å (mean 1.94 Å) and 2.063 (11) to 2.154 (12) Å (mean 2.12 Å), respectively.

the remaining ring ($Li_{123}$–$O_{14}$–$C_{11}$–$C_{12}$–$N_{13}$) is intermediate in nature. With respect to the $C_2$-related $Li_{123}$–$N_{13}$ and $Li_{314}$–$N_{33}$ rings, the C-methyl and phenyl groups are pseudoaxial and pseudoequatorial, respectively, whereas for the $Li_{234}$–$N_{23}$ and $Li_{412}$–$N_{43}$ rings, the orientations of these substituents are interchanged.

As will be seen below, differences between the solution structures of these diastereomers are much more striking. The solid-state structures are valuable in demonstrating the close similarity between these lithium-bridged tetramers and a variety of other published structures. However, although we shall provide strong

evidence for lithium chelation in solution, the solution structures of these alkoxides are very complex in THF. Even in benzene and dioxane, where the solution structures appear to be more straightforward, there is no compelling reason to believe that even the tetrameric aggregates have the same structures as those found in the solid state.

**Solution Structures of the Lithium Alkoxides in THF.** The lithium alkoxides were found to exist as either hexamers or tetramers in THF at 37 °C by VPO (Table V). However, each [$^6$Li] alkoxide exhibited several $^6$Li NMR resonances at −80 °C that coalesced into one or two peaks as the temperature was raised to 37 °C. (See Figures 3 and 4.) These multiple resonances are indicative of nonequivalent $^6$Li nuclei, but it is still unclear whether these nonequivalent $^6$Li nuclei belong to different aggregated species or to one very complex aggregate in solution at −80 °C.

There is a striking similarity between the spectra shown in Figures 3 and 4 and the $^7$Li NMR spectra obtained by Snaith and co-workers[40] for "ladder" lithium amide compounds in toluene-$d_8$. While it is premature to propose solution structures for the alkoxides in THF, there is a strong possibility that they may exist as some variant of the "ladder" arrangements. At the very least, the solution structures of these lithium alkoxides in THF (the most synthetically relevant solvent) are very complex.

Intriguing differences were observed between the $^6$Li NMR spectra of the diastereomeric ephedrine compounds in THF-$d_8$. For lithium pseudoephedrate (**5a**), four $^6$Li resonances were observed, and the spectra at −80, −40, and 0 °C were identical. (See Figure 3.) Its diastereomer, lithium ephedrate (**6a**), also showed four $^6$Li resonances at −80 °C, but these peaks coalesced into one at −40 °C. (See Figure 4.) Since the solution structures of the alkoxides are complex in THF, it is impossible to explain these diastereomeric differences, although the spectra provide dramatic evidence for how greatly the solution structures of the alkoxides may be affected by the stereochemistry of the ephedrine derivative. These observations may help to illuminate the formation of stereospecific products from diastereomeric transition structures in the future.

**Dioxane.** The lithium alkoxides were found to exist as either hexamers or tetramers in dioxane by VPO (37 °C) and cryoscopy (13 °C) (Table V). The aggregation states of lithium ephedrate (**6a**) and 2-methoxy-1-phenyl-1-propoxide (**9a**) are either hexamers or tetramers in benzene; the colligative property techniques did not differentiate between these two aggregation states.

The variable-temperature $^6$Li NMR spectra for all the [$^6$Li] alkoxides consisted of only one resonance, whose chemical shift did not change as a function of temperature. This indicates that no equilibrium between different aggregates occurs in solution and that the actual aggregate must have a high degree of symmetry since all the $^6$Li nuclei are magnetically equivalent.

The vicinal coupling constant ($^3J$) was measured to decide whether chelation occurred in solution. All the $^3J$ values in Table VI are similar to those obtained for the alcohols (Table III) and are consistent with an alkoxide conformation in which intramolecular lithium chelation occurs. Despite repeated attempts, a $^3J$ value could not be obtained for lithium 2-methoxy-1-phenyl-1-propoxide in either benzene or dioxane since all the $^1$H NMR spectra were poorly resolved.

Further detailed structural information was obtained with $^6$Li-$^1$H NOE NMR spectroscopy. The 2D $^6$Li-$^1$H NOE NMR spectrum for [$^6$Li] pseudoephedrate (**5a**) in dioxane-$d_8$ at 13 °C is shown in Figure 5. The most striking features of this spectrum are the very well-resolved amino proton resonance at −0.3 ppm and its strong NOE crosspeak to the $^6$Li resonance. The latter feature indicates that the interatomic distance between the amino proton and the $^6$Li ion is very small.

In a previous study,[41] it was found that a close spatial proximity between a proton and a lithium ion ("an agostic interaction"[42]) resulted in pronounced *downfield* shifts in the $^1$H NMR spectrum. In lithium pseudoephedrate, the amino proton of the alkoxide was found to lie at −0.3 ppm, which is 1 ppm upfield from its chemical shift in the alcohol. This upfield shift may be explained if one imagines that the short Li-H distance also suggests that the proton is very close to the nitrogen's lone pair of electrons, which would effectively shield the amino proton nucleus.

The observation of the short Li-H distance for the amino proton also is consistent with solid-state and experimental evidence for short interatomic distances between the lithium cation of enolates and the amino proton of secondary amines.[43] An X-ray crystallographic structure of lithium pseudoephedrate would provide much more information about the potential structure for this compound, including the Li-H interatomic distance. However, the lithium pseudoephedrate crystals that precipitated from benzene decomposed into a form that was not suitable for diffraction analysis at temperatures above 6 °C.

The 2D $^6$Li-$^1$H NOE NMR spectrum of [$^6$Li] ephedrate (**6a**) in dioxane-$d_8$ at 13 °C is shown in Figure 6. There are several differences between this spectrum and that of lithium pseudoephedrate. (See Figure 5.) The amino proton of lithium ephedrate lies at 0.7–0.8 ppm and does not show a NOE crosspeak to $^6$Li. Only three protons have crosspeaks to $^6$Li, including those of the methyl group at the 2-position, which are the only ones that do not exhibit a NOE crosspeak in lithium pseudoephedrate. While the signal-to-noise ratio of Figure 6 (ephedrate) is considerably less than that of Figure 5 (pseudoephedrate), these spectroscopic differences between the two diastereomeric alkoxides are real. There do appear to be differences in the solution conformations of the alkoxides which result from either the different stereochemical relationships of the phenyl and methyl groups in the two ephedrine molecules and/or different aggregation states.

**Benzene.** Lithium *sec*-phenethanolate, pseudoephedrate, and ephedrate are hexamers in benzene by VPO and cryoscopy. (See Table V.) The other alkoxides are tetramers. The variable-temperature $^6$Li NMR spectra of the [$^6$Li] alkoxides in benzene-$d_6$ show only one resonance, whose chemical shift is invariant to temperature. The tetrameric aggregates of lithium *N*-methylpseudoephedrate (**7a**) and *N*-methylephedrate (**8a**) in benzene solution are presumed to be similar to the solid-state tetramers that were found by X-ray crystallography. (See Figure 7 and ref 16.)

The conformations of the alkoxides were determined by $^1$H NMR with the vicinal coupling constant ($^3J$). (See Table VI.). The $^3J$ values of the alkoxides are similar to those of the corresponding alcohols (Table III), and all are consistent with conformations where intramolecuar lithium chelation occurs.

We offer no explanation for why the aggregation states of lithium pseudoephedrate, ephedrate, and *sec*-phenethanolate differ in benzene ($n = 6$) and dioxane ($n = 4$). Dioxane interaction with *sec*-phenethanolate could be responsible for the reduction of the hexamer to the tetramer. Indeed, THF interacts with this lithium alkoxide in benzene as shown by VPO titration (Figure 2).

(38) Only one $^6$Li resonance was observed in the variable-temperature $^6$Li NMR spectra.

(39) The tetramer $[C_{11}H_{16}LiNO]_4 \cdot C_6H_6$ depicted in Figure 7 crystallizes in the orthorhombic system, space group $P2_12_12_1(D_2^4)$ with $a = 18.428$ (2) Å, $b = 24.174$ (2) Å, $c = 11.138$ (1) Å (from 25 orientation reflections, $40° < \theta < 44°$), $V = 4962$ (1) Å$^3$, $Z = 4$, $d_{calcd} = 1.096$ g cm$^{-3}$, $\mu$(Cu K$\alpha$) = 4.9 cm$^{-1}$. Intensity data ($+h,+k,+l$: 5618 nonequivalent reflections; $\theta_{max} = 75°$) were recorded on an Enraf-Nonius CAD-4 diffractometer (Cu K$\alpha$ radiation, $\lambda = 1.5418$ Å; graphite monochromator; $\bar{\omega}$-$2\theta$ scans). The crystal structure was solved by direct methods (MULTAN11/82). Full-matrix least-squares refinement of atomic parameters (anisotropic C, Li, N, O; fixed H contributions) converged (maximum shift $0.01\sigma$) at $R = 0.054$ ($R_w = 0.067$, GOF = 1.34) over 2567 reflections with $I > 2.0\sigma(I)$. Further details are provided as supplementary material.

(40) Armstrong, D. R.; Barr, D.; Clegg, W.; Hodgson, S. M.; Mulvey, R. E.; Reed, D.; Snaith, R.; Wright, D. S. *J. Am. Chem. Soc.* **1989**, *111*, 4710–4727.

(41) Bauer, W.; Fiegel, M.; Muller, G.; Schleyer, P. v. R. *J. Am. Chem. Soc.* **1988**, *110*, 6033–6046.

(42) Brookhart, M.; Green, M. H. *J. Organomet. Chem.* **1983**, *250*, 395–408.

(43) For leading references and an excellent discussion, see: pp 1638–1639 of ref 9a.

**Table XI.** Enthalpies of Stabilization ($\Delta H_{stab}$) for Lithium 2-Substituted-1-phenyl-1-propoxides in Benzene (6 °C) and Dioxane (13 °C)[a]

| compound | $-\Delta H_{stab}$ (kcal/mol) benzene[b] | dioxane[b] |
|---|---|---|
| pseudoephedrate (**5**) | 10.1 ± 1.6 | 6.9 ± 0.7 |
| ephedrate (**6**) | 11.1 ± 1.6 | 8.3 ± 1.5 |
| *N*-methylpseudoephedrate (**7**) | 6.4 ± 1.9 | *c* |
| *N*-methylephedrate (**8**) | 8.4 ± 1.2 | 6.9 ± 1.5 |
| *syn/anti*-2-methoxy-1-phenyl-1-propanol (87:13) (**9**) | 6.3 ± 1.4 | 7.1 ± 0.5 |
| *syn/anti*-2-(isopropylthio)-1-phenyl-1-propanol (88:12) (**10**) | 7.2 ± 1.3 | 5.2 ± 0.7 |

[a] Errors are given at the 95% confidence limit. [b] Calculated with eq 1 and the $\Delta H_{dep}$ value for 2-methyl-1-phenyl-1-butanol. [c] This compound was insoluble in dioxane.

However, dioxane interaction with the lithium cations of the ephedrates is unlikely since lithium chelation by the amino nitrogen occupies the fourth lithium coordination site.

**Solution Structures of LHMDS.** A complete analysis of the thermochemical results must include the energetic contributions from the lithium amide base (LHMDS) and the amine that results as a deprotonation product (HMDS). In any given solvent the energies of LHMDS and HMDS can be considered as constants for each alkoxide deprotonation measurement, but, where comparisons between data obtained in different solvents are made, the solution structure of LHMDS in each solvent is important. LHMDS is dimeric in benzene and dioxane and exists in a monomer–dimer equilibrium in THF.

**Thermodynamics.** The p$K_a$'s of the ephedrine alcohols in $Me_2SO$ were determined at 25 °C with the Bordwell indicator method as listed in Table I. There is no significant difference beween the acidities of these diastereomeric alcohols in this polar nonhydroxylic solvent. The p$K_a$'s of the ephedrine alcohols are close to published values for methyl alcohol, 29.0; isopropyl alcohol, 30.25; and *tert*-butyl alcohol, 32.2.[44] One would not expect β-substituted amino groups to have much effect on the thermodynamic acidity.

**THF.** Since the lithium alkoxides had very complex solution structures in THF, the $\Delta H_{dep}$ data cannot be interpreted in detail; although all the alcohols were monomeric in this solvent, the structures of the lithium alkoxides are probably different. Still, general trends can be discussed. Table VIII gives the $\Delta H_{dep}$ data for the ephedrine alcohols in THF at 25 °C with Li, Na, and KHMDS. The $\Delta H_{dep}$ values for the alcohols decreased as the cation was changed from Li to Na to K. This trend can be predicted from the ion-pairing abilities of the alkali cations[45] and the decreasing charge density as the ionic radius increases. How aggregation affects this general trend is unclear since the aggregation states of the sodium and potassium alkoxides were not determined. No clear trends in the $\Delta H_{dep}$ values between individual alcohols with the same base were observed.

The high exothermicity of the $\Delta H_{dep}$ value for *sec*-phenethanol relative to the other nonchelated alcohols cannot be explained at this time. This trend was also observed in dioxane (Table IX), but it must be stressed again that the solution structure of lithium *sec*-phenethanolate is very complex in THF and may involve an equilibrium between several aggregated species.

**Dioxane.** The $\Delta H_{dep}$ values obtained for the alcohols with LHMDS in dioxane at 13 °C are listed in Table IX. The nonchelatable alcohols have $\Delta H_{dep}$ values ranging from −13.2 to −14.1 kcal/mol. The $\Delta H_{dep}$ values for the chelated alcohols range from −18.8 to −21.8 kcal/mol. The estimated stabilization energies ($\Delta H_{stab}$) of the chelated alkoxides relative to the nonchelatable model 2-methyl-1-phenyl-1-butanol (**4**) are listed in Table XI and range from −5.2 to −8.3 kcal/mol. (These values were estimated with eq 1 below.) There is little difference in the $\Delta H_{stab}$ values for the chelatable alcohols, suggesting that for these structures the oxygen, nitrogen, and sulfur-based chelating groups stabilize the lithium alkoxides equally well.

*sec*-Phenethanol is anomalous, as in THF, since its $\Delta H_{dep}$ value is −20 kcal/mol. The extra thermodynamic stability of this alkoxide relative to the other nonchelatable models might be attributed to the interaction of one or more THF or dioxane molecules with a lithium cation of the alkoxide aggregate. THF was shown to interact with lithium *sec*-phenethanolate in benzene by VPO titration. (See Figure 2.) It is reasonable that dioxane also would interact with the alkoxide, effectively stabilizing its aggregate, and thereby increasing the exothermicity of the deprotonation reaction. The interaction with dioxane is large enough to stabilize the alkoxide aggregate to the same extent as does intramolecular lithium chelation. (The $\Delta H_{dep}$ values for *sec*-phenethanol and the chelatable alkoxides are similar.) The above interpretation implies that increased steric bulk at the 2-position of the other nonchelatable alkoxides reduces the interaction of dioxane with these alkoxides. These are still preliminary hypotheses since the aggregation states of the 2-substituted nonchelatable alkoxides were not determined.

**Benzene.** The $\Delta H_{dep}$ values obtained for the alcohols with LHMDS in benzene at 6 °C are listed in Table X. The nonchelatable models had $\Delta H_{dep}$ values, ranging from −26.2 to −27.6 kcal/mol. In benzene, the value for *sec*-phenethanol (−26.6 kcal/mol) was similar to that of the other nonchelatable alcohols, which further supports the proposed interaction of dioxane with the lithium *sec*-phenethanolate aggregate as responsible for the relatively high exothermicity of the deprotonation reaction for this alcohol in pure dioxane.

The chelatable alcohols had $\Delta H_{dep}$ values ranging from −33.5 to −38.2 kcal/mol. Heats of deprotonation for the ephedrine alcohols were more exothermic than for the *N*-methylephedrines or the methoxy- or isopropylthio-substituted alcohols by 2.0–4.7 kcal/mol. This is probably because the lithium ephedrates are hexameric, whereas the other alkoxides are tetrameric. The $\Delta H_{stab}$ values for the chelated alkoxides ranged from −6.3 to −11.1 kcal/mol in benzene. (See Table XI.)

The $\Delta H_{dep}$ values are 13–15 kcal/mol more exothermic in benzene than they are in dioxane. This large effect can be attributed to different solution structures of LHMDS in the two solvents. Although LHMDS was dimeric in both dioxane and benzene, dioxane may interact with the lithium cation in the aggregate and stabilize it relative to the less stabilized dimer in benzene. The THF-[46] and diethyl ether[47]-solvated LHMDS dimers have been reported in the solid state.

The stabilization enthalpies measured in both benzene and dioxane are in good agreement with experimental values of Beak, 8.3 kcal/mol,[11] Klumpp, 3.6–9.8 kcal/mol,[12] and the calculated values of Schleyer, 10.2–13.1 kcal/mol.[13c]

**Steric and Hydrogen-Bonding Energies.** One might like to derive an enthalpy of chelational stabilization ($\Delta H_{stab}$) simply from the difference between the heat of deprotonation of a chelatable β-substituted propanol and a nonchelatable analogue as shown in eq 1.

$$\Delta H_{stab} = \Delta H_{dep}(\text{chelatable}) - \Delta H_{dep}(\text{nonchelatable}) \quad (1)$$

As observed in Table XI, the enthalpies of chelational stabilization obtained with eq 1 are fairly large and fall within the range of lithium chelation energies for several analogous published systems.[11-13] However, it must be emphasized that no more than a rather rough interpretation of the results is in order.

If nothing more were involved than replacing a hydroxyl proton with a lithium for two compounds which were exactly alike in every way except for the presence of a chelatable electronegative atom at the β-position of one of them, it would be appropriate to analyze each case in-depth. However, steric strains and conformation energies vary throughout both the chelatable and nonchelatable

(44) Bordwell, F. G. *Acc. Chem. Res.* **1988**, *21*, 456–463.
(45) Arnett, E. M.; DePalma, V.; Maroldo, S.; Small, L. S. *Pure Appl. Chem.* **1979**, *51*, 131–137, and references therein.
(46) Englehardt, L. M.; Jolly, B. S.; Punk, P. C.; Raston, C. L.; Skelton, B. W.; White, A. H. *Aust. J. Chem.* **1986**, *39*, 133.
(47) Lappert, M. F.; Slade, M. J.; Singh, A.; Atwood, J. L.; Rogers, R. D.; Shakir, R. *J. Am. Chem. Soc.* **1983**, *105*, 302.

series from one compound to another. Furthermore, as has been demonstrated by several infrared studies of the ephedrine alcohols,[34] considerable hydrogen bonding is present in the initial alcohol state before deprotonation occurs, and this probably also holds for the other chelatable systems. (See Table III.) Therefore, in every case where the initial alcohol is stabilized by hydrogen bonding, the actual $\Delta H_{stab}$ must be several kcal/mol higher than that derived experimentally through eq 1 because the stabilization factor in the initial state is not present in the nonchelatable model compound.

Although there is no ideal method available for correcting each compound to remove the effects of steric strain and hydrogen bonding, we have used Allinger's MM2(87) program, which allows for an estimation of energetic terms as they would apply to the molecule in the gas phase with no intermolecular association or solvent interactions. Since we have shown that the alcohols were similarly unassociated in the three solvents used here, only small errors due to differential hydrogen bonding would be apt to result by transfer from the gas phase to solution.

The MM2(87) program not only yields energetic terms but also calculates the geometry of the most thermodynamically favored conformation of the molecule. The conformations of the ephedrine alcohols in solution have been determined experimentally with $^1$H NMR and the vicinal coupling constant ($^3J$). (See Table III.) These conformations (in terms of $^3J$) show that intramolecular hydrogen bonding is highly probable for each alcohol in all solvents.

The total minimized steric energies ($E_{min}$) calculated with MM2(87) are given in Table II. Nonchelatable alcohols were synthesized having methyl, ethyl, and isopropyl substituents at the 2-position to provide more accurate steric models for the chelatable alcohols. There was a 4 kcal/mol difference in $E_{min}$ from *sec*-phenethanol to 2-methyl-1-phenyl-1-butanol. The $E_{min}$ values for the chelatable alcohols ranged from 1.5 to 9.4 kcal/mol, with *N*-methylephedrine having the highest value.

For alcohols **5**, **6**, and **10**, the similarity of the $E_{min}$ values of the nonchelatable and chelatable alcohols allows the simple thermodynamic analysis presented in eq 1 to be used. There are considerable differences between the $E_{min}$ values for alcohols **7–9** and the nonchelatable models, and the values of $\Delta H_{stab}$ obtained with eq 1 must be regarded only as estimates of the true stabilization enthalpies.

**Mechanistic Implications.** The goal of these studies was not to determine the mechanism(s) directly for any asymmetric reactions involving lithium chelation by kinetics. Instead, our approach was to examine compounds that would model the proposed lithium-chelated transition states of some asymmetric syntheses. Then, fundamental studies could be performed to determine, first, if lithium chelation really occurred in these compounds under "synthetic conditions", and, secondly, how the experimental conditions (e.g., solvent and temperature) affected chelation.

Since chelation was observed in solution and in the solid state, these results provide further support for the chelated transition states that have been proposed to be responsible for asymmetric induction in various synthetic reactions[1,17,18] over the last 25 years. The familiar issue of monomeric vs aggregated transition states also applies since all the lithium alkoxides were hexamers or tetramers in solution.

The solution structures of the alkoxides in THF (the solvent used most in these types of synthetic reactions) were very complex and could not be elucidated at this time. The complexities of these aggregated structures should render any future mechanistic studies very difficult and indicate that caution must be exercised when proposing mechanisms of diastereoselective or asymmetric reactions involving potentially lithium-chelated molecules.

The presence of a chelating group clearly results in thermodynamic stabilization of the alkoxide aggregates relative to their nonchelatable analogues. This stabilization energy is substantial, amounting to 5–11 kcal/mol per alkoxide molecule, or 20–66 kcal/mol when the tetrameric or hexameric chelated and nonchelatable aggregates are compared! The thermodynamic stabilization of the chelated aggregates that were measured also provides direct support for proposed lithium-chelated transition states and suggests that the driving force for chelation is thermodynamic.

It is surprising that the nature of the chelating group (O, N, or S based) did not have more of an effect on the $\Delta H_{stab}$ measured. It could have been predicted based on hard soft acid base theory[48] that the methoxy substituent would have chelated better with lithium than either the nitrogen- or sulfur-containing substituents.

Significant differences in the $^6$Li and $^1$H NMR spectra were observed for the lithium ephedrates when the configuration between the phenyl and 2-methyl groups was changed from syn to anti. At this time, it is not known how much the solution structures of diastereomeric alkoxides differ. However, it is important to point out that despite the differences between the solution structures of the alkoxides, the $\Delta H_{stab}$ values varied by only 1–3 kcal/mol.

As the actual mechanisms of lithium-chelated asymmetric reactions are studied in the future, it may be found that stereochemical differences in the reactant molecules (which are often cited as the key elements for certain stereochemical outcomes) become amplified as the molecules are ordered in aggregated structures. As in the study of the aldol reaction, the exact nature of the reactive species remains unknown, and the mechanism of each reaction may vary as the experimental conditions and substrates are changed.

## Conclusions

The solution structures and heats of formation of potentially lithium-chelated alkoxides were studied in THF, benzene, and dioxane as models for transition structures or intermediates proposed for asymmetric syntheses. The 2-substituted-1-phenyl-1-propoxides were hexamers and tetramers in these solvents, although these aggregates were very complex in THF since multiple $^6$Li resonances were observed at temperatures below −80 °C. Significant differences were observed in the variable-temperature $^6$Li (THF), $^1$H, and 2D $^6$Li–$^1$H NOE (dioxane) NMR spectra between lithium pseudoephedrate (**5a**) and ephedrate (**6a**), which indicate that the solution structures of the two ephedrates differ when the stereochemical relationship between the phenyl and methyl groups is varied from anti to syn.

The conformations of the lithium alkoxides were determined with the vicinal coupling constants, and all were consistent with intramolecular lithium chelation occurring in benzene and dioxane. Additional evidence for lithium chelation was provided by the observation of a short interatomic distance between $^6$Li and the amino proton of lithium pseudoephedrate in dioxane-$d_8$ with HOESY spectroscopy.

Single crystals of lithium *N*-methylpseudoephedrate and *N*-methylephedrate were obtained upon precipitation from 95:5 dioxane/THF and benzene, respectively, and their X-ray crystallographic structures were elucidated. Both alkoxides were tetrameric in the solid-state and lithium chelation by the amino group was observed. The tetrameric structures that are formed in benzene and dioxane are presumed to be similar to these solid-state structures.

The enthalpies of chelational stabilization ($\Delta H_{stab}$) for the 2-substituted alkoxides were estimated with the $\Delta H_{dep}$ of the alcohols with LHMDS. The complexity of the solution structures in THF prevented calculation of the $\Delta H_{stab}$ values in this solvent. The $\Delta H_{dep}$ values for the alkoxides decreased by 8 and 6 kcal/mol as the cation of the disilazide base was changed from Li to Na and Li to K, respectively.

The $\Delta H_{stab}$ values of the alkoxides could be estimated in dioxane and benzene since no equilibria between aggregation states or complex aggregates were observed. These $\Delta H_{stab}$ values ranged from −5.2 to −8.3 kcal/mol in dioxane (13 °C) and from −6.3 to −11 kcal/mol in benzene (6 °C).

Finally, *sec*-phenethanol had surprisingly different $\Delta H_{dep}$ values from the other nonchelatable alcohols in THF and dioxane. This

(48) Pearson, R. G. *Hard and Soft Acids and Bases*; Dowen, Hutchinson, and Ross, Inc.: Stroudsbury, PA, 1978.

is probably due to the interaction of the ether solvent with the lithium cation of the aggregate.

**Acknowledgment.** This work was supported by NSF Grant CHE-8709249 to E.M.A., for which we are most appreciative. We acknowledge Dr. Anthony A. Ribeiro of the Duke Magnetic Resonance Center for his assistance in the implementation of the $^6$Li-$^1$H NOE NMR experiment and Dr. Franklin J. Fisher for initial thermochemical experiments.

**Supplementary Material Available:** Atomic numbering scheme and tables of crystallographic data, atomic positional and thermal parameters, bond lengths and angles, and selected torsion angles for lithium (-)-*N*-methylephedrate benzene solvate (14 pages); listing of observed and calculated structure amplitudes (18 pages). Ordering information is given on any current masthead page.

# Molecular Recognition of Quinones: Two-Point Hydrogen-Bonding Strategy for the Construction of Face-to-Face Porphyrin-Quinone Architectures[1]

**Yasuhiro Aoyama,*[,†,2] Masumi Asakawa,[†] Yuichi Matsui,[†] and Hisanobu Ogoshi*[,‡]**

*Contribution from the Department of Chemistry, Nagaoka University of Technology, Kamitomioka, Nagaoka, Niigata 940-21, Japan, and Department of Synthetic Chemistry, Kyoto University, Sakyo-Ku, Kyoto 606, Japan.* *Received February 18, 1991*

**Abstract:** 5,15-*cis*-Bis(2-hydroxy-1-naphthyl)octaethylporphyrin (**1**) in chloroform selectively binds *p*-quinones via a two-point hydrogen-bonding interaction between the two, convergent hydroxyl groups of host **1** and the two carbonyl moieties of a guest quinone. Upon complexation, the $^1$H NMR resonance and IR absorption for the OH groups undergo a characteristic downfield shift and a shift to lower wavenumber, respectively ($\Delta\delta_{comp}$(OH) = 1.38-2.85 ppm and $\Delta\nu_{comp}$(OH) = 30-102 cm$^{-1}$, depending on the basicities of quinones). The binding constants ($K$) evaluated by $^1$H NMR titration at 298 K decrease in the order anthraquinone (**17**; 2.3 × 10$^2$ M$^{-1}$) > naphthoquinone (**15**; 1.7 × 10$^2$) > benzoquinone (**5**; 5.5 × 10): Those for benzoquinone derivatives are duroquinone (**12**; 4.2 × 10$^2$) > chloranil (**6**; 4.0 × 10$^2$) > fluoranil (**7**; 3.7 × 10$^2$) > 2,5-dichlorobenzoquinone (**8**; 2.2 × 10$^2$) > 2-chlorobenzoquinone (**9**; 1.2 × 10$^2$) > 2,5-dimethylbenzoquinone (**11**; 1.1 × 10$^2$) > 2-methylbenzoquinone (**10**; 8.8 × 10) > benzoquinone (**5**; 5.5 × 10) > 2,3-dimethoxy-5-methylbenzoquinone (**13**; 3.5 × 10) > tetramethoxybenzoquinone (**14**; 7.8). The variation in $K$'s suggests that the strength of hydrogen bonds, direct porphyrin-quinone interaction apparently of a charge-transfer type, and the steric effects of methoxy substituents are important factors. Reference guests such as anthrone (**18**; $K$ = 4.2 M$^{-1}$), *o*-naphthoquinone (**16**; 8.7), and 1,4-cyclohexanedione (**19**; 1.0 × 10) show significantly lower affinities to host **1** than those for the corresponding *p*-quinone counterparts. The resulting **1**-quinone adducts have an estimated face-to-face separation of as short as 3 Å and exhibit porphyrin-quinone $\pi$-$\pi$ interaction as revealed by UV/visible spectroscopy; the longest wavelength absorption band of **1** undergoes either a blue shift or a red shift depending on the electronic property of bound quinone. In addition, the adducts are rendered completely nonfluorescent as a result of an efficient, intracomplex electron transfer from photoexcited **1** to bound quinone. Thus, the abilities of quinones to quench fluorescence of porphyrin **1** are related not with their redox properties but with their abilities to bind to **1**; **6** ≅ **12** > **17** > **8** > **11** > **5**. The present host-guest complexation is discussed from the viewpoint of noncovalent strategy for the construction of biologically significant structures.

Quinone derivatives play an essential role as electron mediators in the charge separation processes in photosynthesis.[3] A variety of *covalently* linked porphyrin-quinone derivatives have been prepared and photoinduced electron transfer therein investigated as models of photosynthetic electron transfer.[4] This is along a typical line of biomimetic chemistry, a popular methodology of which is assembly of supposedly essential components via covalent linkage. In the present work, we have taken a different strategy to construct face-to-face porphyrin-quinone architectures. This is based on *noncovalent interaction*.[5] *cis*-Bis(2-hydroxynaphthyl)porphyrin **1** spontaneously forms such face-to-face adducts with *p*-quinones.[6] We report here on the details of this complexation, focusing upon (1) the structure-stability correlation from the viewpoint of molecular recognition of quinones and (2) the electronic interaction and photoinduced electron transfer in the adducts in relevance to the function of porphyrin-quinone architectures.

Chart I

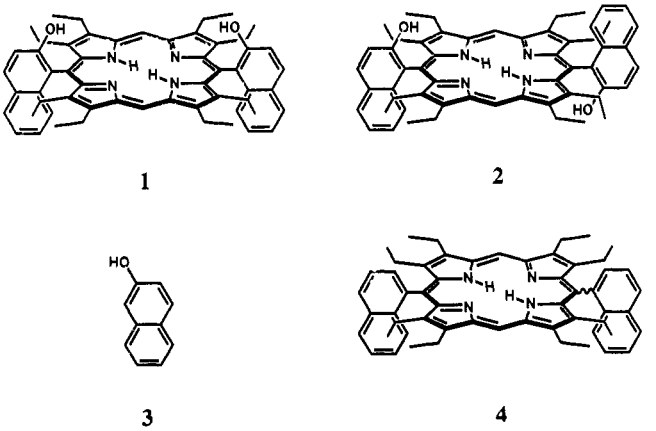


1 2 3 4

## Results and Discussion

**Two-Point Hydrogen-Bonding Fixation of *p*-Quinones.** The interactions of various quinones with 5,15-*cis*-bis(2-hydroxy-1-naphthyl)octaethylporphyrin (**1**) as well as its trans isomer **2**, 2-naphthol (**3**), and dinaphthyl derivative **4** as references in

[†] Nagaoka University of Technology.
[‡] Kyoto University.

(1) Molecular Recognition. 16. Part 15: Kikuchi, Y.; Kato, Y.; Tanaka, Y.; Tol, H.; Aoyama, Y. *J. Am. Chem. Soc.* **1991**, *113*, 1349.

0002-7863/91/1513-6233$02.50/0 